

---

# Negative Feedback Really Matters: Signed Dual-Channel Graph Contrastive Learning Framework for Recommendation

---

Leqi Zheng <sup>1</sup>, Chaokun Wang <sup>1\*</sup>, Zixin Song <sup>1</sup>, Cheng Wu <sup>1</sup>,  
Shannan Yan <sup>1</sup>, Jiajun Zhang <sup>2</sup>, Ziyang Liu <sup>1</sup>

<sup>1</sup>Tsinghua University <sup>2</sup>University of Science and Technology of China  
{zhenglq24, songzx24, wuc22, ysn24, liu-zy21}@mails.tsinghua.edu.cn  
chaokun@tsinghua.edu.cn, zhangjiajun519@mail.ustc.edu.cn

## Abstract

Traditional recommender systems have relied heavily on positive feedback for learning user preferences, while the abundance of negative feedback in real-world scenarios remains underutilized. To address this limitation, recent years have witnessed increasing attention on leveraging negative feedback in recommender systems to enhance recommendation performance. However, existing methods face three major challenges: limited model compatibility, ineffective information exchange, and computational inefficiency. To overcome these challenges, we propose a model-agnostic Signed Dual-Channel Graph Contrastive Learning (SDCGCL) framework that can be seamlessly integrated with existing graph contrastive learning methods. The framework features three key components: (1) a Dual-Channel Graph Embedding that separately processes positive and negative graphs, (2) a Cross-Channel Distribution Calibration mechanism to maintain structural consistency, and (3) an Adaptive Prediction Strategy that effectively combines signals from both channels. Building upon this framework, we further propose a Dual-channel Feedback Fusion (DualFuse) model and develop a two-stage optimization strategy to ensure efficient training. Extensive experiments on four public datasets demonstrate that our approach consistently outperforms state-of-the-art baselines by substantial margins while exhibiting minimal computational complexity. Our source code and data are released at <https://github.com/LQgdwind/nips25-sdcgcl>.

## 1 Introduction

Recommender systems have become integral components of modern digital platforms, significantly influencing user engagement and satisfaction across diverse domains such as e-commerce, social media, and content streaming services. While substantial progress has been made in leveraging positive feedback (e.g., likes, high ratings) for recommendation, the effective utilization of negative feedback (e.g., dislikes, low ratings) remains a critical yet underexplored avenue for enhancing recommendation performance [21, 34, 7, 6].

This disparity is particularly noteworthy given that negative feedback often provides explicit signals about users' preferences and can potentially offer more precise guidance for recommendation refinement than positive feedback alone [22, 52, 43]. As shown in Figure 1, traditional unsigned graphs only capture the existence of positive interactions, whereas sign-aware graphs preserve the polarity of feedback through different edge types, enabling more comprehensive modeling

---

\*Corresponding author

of user preferences. Therefore, the recent research [34, 29, 6, 43] has increasingly focused on negative feedback in recommender systems. However, these studies face three major challenges:

(1) **Limited Model Compatibility**: Most existing methods design specialized models for processing signed feedback [49, 43], making them incompatible with recent advances in graph-based recommendation models. This specialization prevents them from benefiting from state-of-the-art techniques like graph contrastive learning, which have demonstrated remarkable success in unsigned recommendation scenarios. (2) **Limited Information Exchange**: Most existing methods treat negative feedback as auxiliary signals, failing to fully exploit its potential [34, 6]. These methods primarily focus on positive feedback while only partially utilizing negative feedback, resulting in an incomplete understanding of user preferences and suboptimal recommendations. (3) **Limited Training Strategy**: Existing methods either process the full signed graph during training or rely solely on sampled feedback [49, 6], failing to strike a balance between comprehensive learning and training efficiency.

Motivated by the aforementioned issues, we propose a novel Signed Dual-Channel Graph Contrastive Learning (SDCGCL) framework that revolutionizes the integration of negative feedback in recommendation systems. The framework consists of three key components: (1) a Dual-Channel Graph Embedding that separately processes positive and negative graphs, (2) a Cross-Channel Distribution Calibration mechanism to maintain structural consistency between channels, and (3) an Adaptive Prediction Strategy that effectively combines signals from both channels. To further enhance the framework’s effectiveness, we present the Dual-channel Feedback Fusion (DualFuse) model, which implements a dual-channel graph encoder and cross-channel graph fusion, enabling simultaneous processing of positive and negative feedback patterns. To address training efficiency, we also propose a two-stage optimization strategy that combines comprehensive learning on full graphs with efficient training on strategically sampled subgraphs. This approach is theoretically proven to preserve recommendation quality.

The main contributions of this work are summarized as follows:

- **Model-Agnostic Framework**: We propose SDCGCL, a model-agnostic framework that can be seamlessly incorporated into existing graph contrastive learning methods, overcoming the compatibility limitation of current signed recommendation approaches (Section 2.1).
- **Cross-Channel Information Fusion**: We design DualFuse, a novel model featuring dual-channel encoding and cross-channel fusion mechanisms to enable effective information exchange between positive and negative feedback patterns while preserving channel-specific characteristics (Section 2.2).
- **Two-Stage Training Strategy**: We develop a two-stage optimization strategy combining comprehensive learning on full graphs with efficient training on strategically sampled subgraphs, with theoretical guarantees for both training effectiveness and efficiency (Section 3).
- **Experimental Validation**: Extensive experiments on four public datasets demonstrate that our approach consistently outperforms the state-of-the-art baselines by substantial margins, while achieving the superior computational efficiency with faster convergence (Section 4).

## 2 Model Design

In this section, we propose two key novel techniques: (1) a model-agnostic **Signed Dual-Channel Graph Contrastive Learning** (SDCGCL) framework (Section 2.1), and (2) a **Dual-Channel Feedback Fusion** (DualFuse) model specifically designed to complement this framework (Section 2.2).

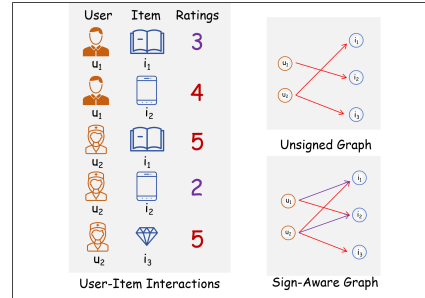


Figure 1: Comparison between unsigned graph and sign-aware graph in recommender systems. Left: User-item interactions with explicit ratings showing both positive (4-5) and negative (1-3) feedback. Right: Unlike unsigned graphs (top), sign-aware graphs (bottom) preserve feedback polarity through different edge types.

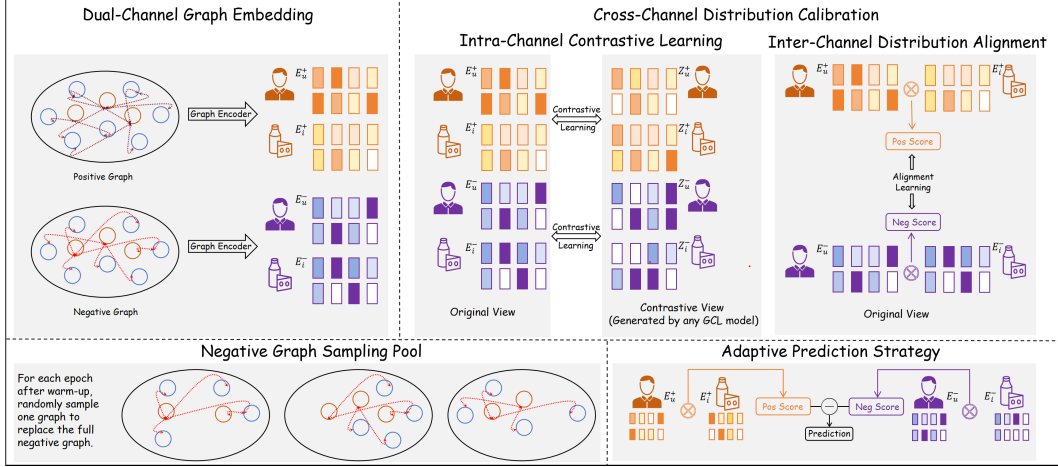


Figure 2: Overview of the SDCGCL framework. The framework consists of three main components: (1) Dual-Channel Graph Embedding, (2) Cross-Channel Distribution Calibration, and (3) Adaptive Prediction Strategy. A negative graph sampling pool (bottom left) enables efficient training optimization.

## 2.1 Model-agnostic SDCGCL Framework

In this subsection, we propose our model-agnostic **Signed Dual-Channel Graph Contrastive Learning** (SDCGCL) framework, which effectively leverages both positive and negative user feedback for recommendation tasks. The SDCGCL framework consists of three key components: dual-channel graph embedding, cross-channel distribution calibration, and an adaptive prediction strategy, as illustrated in Figure 2.

### 2.1.1 Dual-Channel Graph Embedding

To effectively leverage both positive and negative feedback, our SDCGCL framework independently propagates the positive and negative interaction graphs using graph contrastive learning techniques.

For each channel, we independently encode the user and item embeddings through a message propagation function  $f(\cdot)$  and a dropout strategy function  $p(\cdot)$ , which can be instantiated with any suitable GNN backbone. The embeddings are updated over  $L$  layers:

$$\mathbf{e}_{u,l}^+ = f(p(\hat{\mathbf{A}}^+), \mathbf{e}_{u,l-1}^+), \quad \mathbf{e}_{u,l}^- = f(p(\hat{\mathbf{A}}^-), \mathbf{e}_{u,l-1}^-) \quad (1)$$

where  $\mathbf{e}_{u,l}^+$ ,  $\mathbf{e}_{u,l}^-$  denote layer  $l$  embeddings,  $\mathbf{e}_{i,l-1}^+$ ,  $\mathbf{e}_{i,l-1}^-$  represent layer  $l-1$  item embeddings, and  $\hat{\mathbf{A}}^+$ ,  $\hat{\mathbf{A}}^-$  are normalized adjacency matrices in positive/negative channels. After  $L$  layers of propagation, we obtain the final graph embeddings:

$$\mathbf{E}_u^+ = \text{AGG} \left( \{\mathbf{e}_{u,l}^+ : l \leq L\} \right), \quad \mathbf{E}_u^- = \text{AGG} \left( \{\mathbf{e}_{u,l}^- : l \leq L\} \right) \quad (2)$$

where  $\mathbf{E}_u^+$  and  $\mathbf{E}_u^-$  denote final graph embeddings in positive/negative channels, and  $\text{AGG}(\cdot)$  denotes a function that aggregates embeddings from different layers, such as mean pooling or concatenation.

To generate contrastive views for contrastive learning, we apply the base model’s augmentation mechanism to obtain augmented embeddings at a designated layer  $l^*$ :

$$\mathbf{z}_{u,l^*}^+ = \phi \left( \hat{\mathbf{A}}^+, \mathbf{e}_{u,l}^+, \mathbf{X}, \boldsymbol{\theta} \right), \quad \mathbf{z}_{u,l^*}^- = \phi \left( \hat{\mathbf{A}}^-, \mathbf{e}_{u,l}^-, \mathbf{X}, \boldsymbol{\theta} \right) \quad (3)$$

where  $\phi(\cdot)$  represents the base model’s specific augmentation mechanism,  $\mathbf{X}$  denotes optional node features, and  $\boldsymbol{\theta}$  contains augmentation-specific parameters (e.g., dropout rates). The final contrastive embeddings are then obtained by aggregating the augmented embeddings:

$$\mathbf{Z}_u^+ = \text{AGG}^* \left( \{\mathbf{z}_{u,l^*}^+\} \right), \quad \mathbf{Z}_u^- = \text{AGG}^* \left( \{\mathbf{z}_{u,l^*}^-\} \right) \quad (4)$$

where  $\text{AGG}^*(\cdot)$  is the contrastive view aggregator. Similar notations apply to items with embeddings  $\mathbf{E}_i^+$ ,  $\mathbf{E}_i^-$ ,  $\mathbf{Z}_i^+$  and  $\mathbf{Z}_i^-$ .

### 2.1.2 Cross-Channel Distribution Calibration.

To effectively integrate information from both positive and negative feedback channels, our framework employs a cross-channel distribution calibration mechanism, which achieves the information integration through two components: intra-channel contrastive learning and inter-channel distribution alignment.

**Intra-Channel Contrastive Learning.** Given that user preferences exhibit inherent structure within both positive and negative interactions, we first employ channel-specific contrastive learning to capture these underlying patterns. For the positive channel, we optimize:

$$\min_{(u,i) \in \mathcal{G}^+} -\{f^*(\mathbf{E}_u^+, \mathbf{Z}_u^+) + f^*(\mathbf{E}_i^+, \mathbf{Z}_i^+) - \sum_{\substack{(u',i') \in \mathcal{G}^+ \\ u' \neq u, i' \neq i}} \left( \frac{f^*(\mathbf{E}_u^+, \mathbf{Z}_{u'}^+)}{|\mathcal{U}| - 1} + \frac{f^*(\mathbf{E}_i^+, \mathbf{Z}_{i'}^+)}{|\mathcal{I}| - 1} \right) \} \quad (5)$$

Here, the first two terms  $f^*(\mathbf{E}_u^+, \mathbf{Z}_u^+)$  and  $f^*(\mathbf{E}_i^+, \mathbf{Z}_i^+)$  maximize agreement between original embeddings and their augmented views, encouraging robustness to perturbations. Similarly, for the negative channel:

$$\min_{(u,i) \in \mathcal{G}^-} -\{f^*(\mathbf{E}_u^-, \mathbf{Z}_u^-) + f^*(\mathbf{E}_i^-, \mathbf{Z}_i^-) - \sum_{\substack{(u',i') \in \mathcal{G}^- \\ u' \neq u, i' \neq i}} \left( \frac{f^*(\mathbf{E}_u^-, \mathbf{Z}_{u'}^-)}{|\mathcal{U}| - 1} + \frac{f^*(\mathbf{E}_i^-, \mathbf{Z}_{i'}^-)}{|\mathcal{I}| - 1} \right) \} \quad (6)$$

**Inter-Channel Distribution Alignment** While maintaining channel-specific information is important, the excessive divergence between positive and negative embedding spaces can hinder effective integration. We propose an inter-channel distribution alignment mechanism that enforces structural consistency while preserving distinctive features:

$$\min_{u \in \mathcal{U}} \left\{ \sum_{(u,i) \in \mathcal{G}^+} g^* \left( \sum_{(u,j) \in \mathcal{G}^-} \frac{\mathbf{E}_u^+ \circ \mathbf{E}_i^{+\top}}{|\mathcal{N}_u^+|}, \sum_{(u,j) \in \mathcal{G}^-} \frac{\mathbf{E}_u^- \circ \mathbf{E}_j^{-\top}}{|\mathcal{N}_u^-|} \right) \right\}, \min_{i \in \mathcal{I}} \left\{ \sum_{(u,i) \in \mathcal{G}^+} g^* \left( \sum_{(v,i) \in \mathcal{G}^-} \frac{\mathbf{E}_v^+ \circ \mathbf{E}_i^{+\top}}{|\mathcal{N}_i^+|}, \sum_{(v,i) \in \mathcal{G}^-} \frac{\mathbf{E}_v^- \circ \mathbf{E}_i^{-\top}}{|\mathcal{N}_i^-|} \right) \right\} \quad (7)$$

where  $g^*(\cdot, \cdot)$  represents a distribution difference measure between positive and negative channels. The first equation aligns user-centric patterns, while the second addresses item-centric alignments, with normalized interaction scores reflecting neighborhood aggregations.

### 2.1.3 Adaptive Prediction Strategy

After obtaining the calibrated embeddings from both channels, we adopt an adaptive prediction strategy to combine them for final recommendation. The predicted preference score  $\hat{y}_{u,i}$  for user  $u$  and item  $i$  is computed by balancing the contributions from the positive and negative embeddings:

$$\hat{y}_{u,i} = (1 + k) \mathbf{E}_u^+ \circ \mathbf{E}_i^{+\top} - k \mathbf{E}_u^- \circ \mathbf{E}_i^{-\top}, \quad (8)$$

where  $k \in [0, 1]$  is a hyperparameter controlling the influence of negative feedback.

### 2.1.4 Theoretical Analysis

**Theorem 1** (Distribution Instability). *For each node, the negative neighbors  $\mathcal{N}^-$  have an unstable degree of scale. For users, some only give positive ratings and refrain from commenting on items they dislike, while others are more direct and express their negative ratings openly. Therefore, in signed recommendation graphs, the negative feedback distribution exhibits higher variance than positive feedback, with embedding distributions satisfying:*

$$\begin{aligned} \mathbb{E}[\mathbf{E}_u^+ \circ \mathbf{E}_i^{+\top}] &= \mu, \quad \mathbb{E}[\mathbf{E}_u^- \circ \mathbf{E}_i^{-\top}] = \delta_1 + \mu \\ \text{Var}[\mathbf{E}_u^+ \circ \mathbf{E}_i^{+\top}] &= \sigma^2, \quad \text{Var}[\mathbf{E}_u^- \circ \mathbf{E}_i^{-\top}] = \delta_2 \sigma^2 \end{aligned} \quad (9)$$

where  $\delta_2 \geq 1$  represents the inherent instability of negative feedback.

*Proof Sketch.* We show that without distribution alignment, the prediction expectation contains a bias term  $-k\delta_1$  and inflated variance dependent on  $\delta_2$ . Distribution alignment (Eq. 7) ensures  $\delta_1 \rightarrow 0, \delta_2 \rightarrow 1$ , normalizing the prediction expectation to  $\mathbb{E}[\hat{y}_{u,i}] = \mu$  and simplifying variance to  $(2k^2 + 2k + 1) \cdot \sigma^2$ . The complete proof is provided in Appendix A.1.  $\square$

## 2.2 DualFuse Model

SDCGCL is model-agnostic and can integrate with various graph contrastive learning models like SGL, XSimGCL, and LightGCL [46, 57, 2]. However, these models lack negative feedback utilization, limiting their ability to fully exploit the potential of our framework. To address this inadequate utilization, we propose DualFuse, which implements dual-channel graph encoding and cross-channel fusion of positive and negative graphs, enabling simultaneous learning of both interaction patterns to maximize SDCGCL’s effectiveness.

### 2.2.1 Dual-Channel Graph Encoder

DualFuse employs a dual-channel graph encoder based on LightGCN, with distinct embedding spaces for each channel. Embeddings evolve through layer-wise message propagation within channels, and the final representations are computed via multi-hop connectivity aggregation:

$$\mathbf{E}_u^+ = \frac{\sum_{l=0}^L \sum_{i \in \mathcal{N}_u^+} \frac{\mathbf{e}_{i,l-1}^+}{\sqrt{|\mathcal{N}_u^+| \cdot |\mathcal{N}_i^+|}}}{L+1}, \mathbf{E}_u^- = \frac{\sum_{l=0}^L \sum_{i \in \mathcal{N}_u^-} \frac{\mathbf{e}_{i,l-1}^-}{\sqrt{|\mathcal{N}_u^-| \cdot |\mathcal{N}_i^-|}}}{L+1} \quad (10)$$

where  $\mathbf{E}_u^+$  and  $\mathbf{E}_u^-$  denote final graph embeddings in two channels. Similarly, for item  $i$ , we can obtain  $\mathbf{E}_i^+$  and  $\mathbf{E}_i^-$ .

### 2.2.2 Cross-Channel Graph Fusion

DualFuse leverages an innovative cross-channel graph fusion mechanism where embeddings from each channel create perturbations for the other, enriching representations while preserving channel-specific patterns, as shown in Figure 3.

At a designated layer  $l^*$ , we generate contrastive views by introducing structured perturbations derived from the opposite channel. This contrastive views implements the data augmentation function  $\phi(\cdot)$  from Equation 4 through cross-channel fusion:

$$\begin{aligned} \mathbf{Z}_u^+ &= \frac{1}{L+1} \sum_{l=0}^L (\mathbf{e}_{u,l}^+ + \frac{\mathbf{e}_{u,l^*}^-}{\|\mathbf{e}_{u,l^*}^-\|}), \\ \mathbf{Z}_u^- &= \frac{1}{L+1} \sum_{l=0}^L (\mathbf{e}_{u,l}^- + \frac{\mathbf{e}_{u,l^*}^+}{\|\mathbf{e}_{u,l^*}^+\|}) \end{aligned} \quad (11)$$

where  $\mathbf{Z}_u^+$  and  $\mathbf{Z}_u^-$  denote final contrastive embeddings in two channels. Similarly, for item  $i$ , we can obtain  $\mathbf{Z}_i^+$  and  $\mathbf{Z}_i^-$ .

### 2.2.3 Theoretical Analysis

**Theorem 2** (Cross-Channel Information Preservation). *The cross-channel fusion mechanism preserves essential information while maintaining stable gradient flow. For any node  $v \in \mathcal{U} \cup \mathcal{I}$ , at convergence:*

$$\|\nabla_{\mathbf{e}_v^+} \mathcal{L}\| \approx \|\nabla_{\mathbf{e}_v^-} \mathcal{L}\| \quad (12)$$

*Proof Sketch.* By analyzing gradient propagation through the fusion mechanism, we establish that at convergence, when  $\|\frac{\partial \mathcal{L}}{\partial \mathbf{Z}_v^+}\| \approx \|\frac{\partial \mathcal{L}}{\partial \mathbf{Z}_v^-}\|$  and  $\|\mathbf{e}_v^+\| \approx \|\mathbf{e}_v^-\|$ , the gradients in both channels maintain similar magnitudes, ensuring balanced information flow. The detailed derivation is available in Appendix A.2.  $\square$

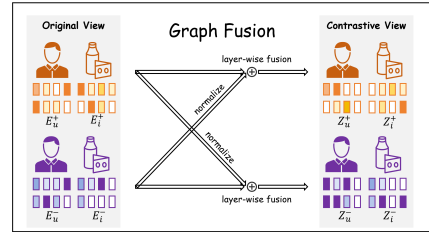


Figure 3: Graph fusion mechanism: Original embeddings from positive (orange) and negative (purple) channels are normalized and fused to generate contrastive views.

### 3 Optimization Design

To effectively train our framework while managing computational complexity, we propose a two-stage optimization strategy that combines comprehensive learning on the full graph with efficient training on strategically sampled subgraphs.

#### 3.1 Two-Stage Optimization Strategy.

**Full-Graph Learning Stage** The first stage operates on the complete signed user-item interaction graph  $\mathcal{G}$ , processing all positive edges  $\mathcal{E}^+$  and negative edges  $\mathcal{E}^-$  simultaneously. The full-graph learning stage is crucial for capturing the complete structure of user preferences and ensuring that no valuable negative feedback information is overlooked during the initial training period.

**Sampled-Graph Learning Stage.** To address the computational challenges posed by large-scale negative interaction graphs while maintaining learning effectiveness, we propose a popularity-guided random walk sampling strategy that is formally presented in Algorithm 1. This strategy carefully constructs subgraphs that preserve the most informative negative feedback patterns.

---

**Algorithm 1:** Popularity-Guided Random Walk Sampling

---

**Input** :Original negative graph  $\mathcal{G}^-$ , sample rate  $\rho$ , walk length  $l$ , temperature  $\tau$

**Output** :Sampled negative graph  $\mathcal{G}^{s-}$

Initialize node degrees  $d_v$  for all  $v \in \mathcal{V}$ ;

Compute importance distribution  $P(v) \leftarrow \frac{\exp(d_v/\tau)}{\sum_{u \in \mathcal{V}} \exp(d_u/\tau)}$ ;

$\mathcal{S} \leftarrow$  Sample  $\rho|\mathcal{V}|$  nodes according to  $P(v)$ ;

Initialize importance scores  $s_v \leftarrow 0$  for all  $v \in \mathcal{V}$ ;

**for** each starting node  $v_0 \in \mathcal{S}$  **do**

$v_t \leftarrow v_0$ ;

**for**  $t = 1$  to  $l$  **do**

        Compute transition probabilities  $P(v_j|v_t) \leftarrow \frac{d_{v_j}}{\sum_{v_k \in \mathcal{N}(v_t)} d_{v_k}}$ ;

        Sample  $v_t$  from  $\mathcal{N}(v_t)$  according to  $P(v_j|v_t)$ ;

        Update importance:  $s_{v_t} \leftarrow s_{v_t} + d_{v_t} \cdot \frac{l-t}{l}$ ;

**end**

**end**

Compute edge importance  $w_{ij} \leftarrow \frac{s_i + s_j}{2}$  for each edge  $(i, j)$ ;

Construct  $\mathcal{G}^{s-}$  with edges where  $w_{ij} > \theta$ ;

**return**  $\mathcal{G}^{s-}$

---

**Theoretical Analysis.** The effectiveness of our two-stage sampling strategy can be theoretically justified through embedding stability bounds:

**Theorem 3** (Two-Stage Stability Bound). *For any node  $v \in \mathcal{U} \cup \mathcal{I}$ , the expected embedding difference satisfies:*

$$\mathbb{E} \left\| \mathbf{e}_v^{(t)} - \mathbf{e}_v^{(t-1)} \right\|_2^2 \leq \begin{cases} C_1/t, & t \leq T_{\text{warm}} \\ C_2(\rho)/t + \epsilon(\rho)/\sqrt{t}, & t > T_{\text{warm}} \end{cases} \quad (13)$$

where  $C_1 := \eta_0^2 L^2 D$  integrates the initial learning rate ( $\eta_0$ ), the Lipschitz constant ( $L$ ) of loss gradients in dense interaction regions ( $\|\mathbf{e}_u - \mathbf{e}_i\|_2 \geq \delta$ ), and the maximum node distance ( $D$ );  $C_2(\rho) := \eta_0^2 \left( L^2 + \frac{\sigma_0^2 + \kappa/\rho}{\rho} \right)$  combines gradient smoothness ( $L^2$ ), base variance ( $\sigma_0^2$ ) from full-graph training, and sparse sampling penalty ( $\kappa/\rho^2$ );  $\epsilon(\rho) := \eta_0 \sqrt{\nu(\rho)}$  encodes information loss where  $\nu(\rho)$  measures divergence between true and sampled negative feedback distributions.

*Proof Sketch.* We analyze each optimization stage separately. In the warm-up phase, embedding differences decay as  $O(1/t)$ . In the sampling phase, the decay follows  $O(1/t) + O(1/\sqrt{t})$ , reflecting the trade-off between sampling efficiency ( $\rho$ ) and variance control ( $\kappa, \nu$ ). The full derivation is provided in Appendix A.3.  $\square$

Table 1: The performance comparison across the methods on four datasets. Baseline best results in **bold**, SDCGCL best results in **bold**\*, second-best underlined. Relative improvement (%) shows the performance gain of SDCGCL-DualFuse over the strongest baseline. \* indicates statistical significance ( $p < 0.01$ ).

Group	Datasets	ML-1M		Yelp		Amazon		ML-10M	
		Models	Recall	NDCG	Recall	NDCG	Recall	NDCG	Recall
U-RS	MF	0.1329	0.1988	0.0334	0.0217	0.0489	0.0364	0.1667	0.2046
	NCF	0.1501	0.2102	0.0359	0.0237	0.0578	0.0427	0.1926	0.2441
	NGCF	0.1630	0.2185	0.0566	0.0475	0.0614	0.0463	0.2162	0.2718
	LightGCN	0.1993	0.2632	0.0662	0.0539	0.0728	0.0631	0.2597	0.3091
	DGCF	0.1768	0.2104	0.0629	0.0504	0.0695	0.0613	0.2241	0.2859
	HyRec	0.1805	0.2181	0.0606	0.0550	0.0658	0.0596	0.2304	0.2805
	GFormer	0.2272	0.2407	0.0597	0.0542	0.0758	0.0672	0.2460	0.3011
	SelfGNN	0.2565	0.2810	0.0791	0.0672	0.0806	0.0724	0.2742	0.3111
	NCL	0.2627	0.2782	0.0699	0.0615	0.0746	0.0676	0.2972	0.3183
	SGL	0.2798	0.3037	0.0746	0.0729	0.0958	0.0694	0.3056	0.3299
	LightGCL	0.2730	0.3035	0.0697	0.0675	0.0967	0.0728	0.3098	0.3231
	XSimGCL	0.2729	0.3087	0.0867	0.0758	0.0963	0.0707	0.3109	0.3371
	IGCL	0.2747	0.3016	0.0692	0.0660	0.0796	0.0661	0.2956	0.3212
S-RS	SiReN	<b>0.3093</b>	0.3338	0.0873	0.0635	0.1017	0.0924	<b>0.3490</b>	<b>0.3583</b>
	SiGRec	0.1937	0.2583	0.0594	0.0499	0.0741	0.0678	0.2302	0.2918
	DFGNN	0.2538	0.3030	0.0728	0.0609	0.0768	0.0705	0.2721	0.3113
	SignGT	0.1635	0.2225	0.0607	0.0536	0.0736	0.0644	0.2366	0.2970
	SBGNN	0.1527	0.2113	0.0621	0.0479	0.0612	0.0548	0.2237	0.2773
	SLGNN	0.1740	0.2370	0.0658	0.0498	0.0617	0.0556	0.2269	0.2912
	SGFormer	0.1877	0.2680	0.0601	0.0459	0.0792	0.0648	0.2344	0.2908
	SIGFormer	0.2995	<b>0.3380</b>	0.0856	0.0777	0.1006	0.0997	0.3217	0.3549
	NFARec	0.2840	0.3212	<b>0.0971</b>	<b>0.0808</b>	<b>0.1136</b>	<b>0.1020</b>	0.3316	0.3442
	Relative improvement (%)	6.110%	9.260%	28.012%	18.689%	18.133%	9.118%	11.748%	7.731%

### 3.2 Multi-Objective Loss Integration

Our training approach integrates three key loss components to effectively capture both positive and negative feedback patterns: (1) recommendation loss based on Bayesian Personalized Ranking for supervision, (2) contrastive learning loss to enhance embedding quality within each channel, and (3) distribution alignment loss to maintain consistent structural information between channels. The final objective function combines these components with balanced weighting parameters:

$$\mathcal{L} = \mathcal{L}_{rec} + \lambda(\mathcal{L}_{cl} + \gamma\mathcal{L}_{dist}) + \eta\|\Theta\|_2^2 \quad (14)$$

where  $\lambda$  controls the overall contribution of the auxiliary objectives,  $\gamma$  weights the distribution alignment constraint, and  $\eta$  is the  $L_2$  regularization coefficient applied to model parameters  $\Theta$ . A comprehensive description of each loss component and their mathematical formulations is provided in Appendix B.

## 4 Experiments

### 4.1 Experimental Setup

We evaluate our method on four publicly available recommendation datasets: Yelp, Amazon, and MovieLens (ML-1M and ML-10M). Following established conventions, we binarize ratings (scores  $\geq 4$  as positive,  $< 4$  as negative). For the performance evaluation, we adopt Recall@20 and NDCG@20 as metrics. We benchmark against 22 state-of-the-art recommendation methods across unsigned and sign-aware recommendation systems. Detailed descriptions of datasets, metrics, baselines, and parameter settings are provided in Appendix C.

### 4.2 Overall Performance

Experimental evaluations demonstrate our approach’s superior performance. As shown in Table 1, DualFuse consistently outperforms all baselines by substantial margins. Compared to the best

unsigned baseline (XSimGCL), our model achieves 20.26% and 19.63% improvements in Recall@20 and NDCG@20 on ML-1M. Against sign-aware methods, DualFuse shows significant gains over NFARec, with Recall@20 improvements of 6.11% (ML-1M), 28.01% (Yelp), and 18.13% (Amazon). SDCGCL framework enhances all integrated methods (see Appendix D.2), validating our dual-channel architecture’s effectiveness.

### 4.3 Ablation Study

#### 4.3.1 Component Analysis

We evaluate our framework through ablation studies on key components. Table 2 shows removing fusion causes 73.80% Recall@20 decrease, while CL and alignment provide 10.45% and 3.49% NDCG@20 improvements respectively. Recommendation loss is critical, with its removal causing 69.94% NDCG@20 degradation and scattered embedding distributions (Details see Appendix D.3 and Figure 4).

Table 2: Performance analysis with different component combinations

Variant	Components				Performance	
	Fusion	CL	Align	Rec	Recall	NDCG
DualFuse	✓	✓	✓	✓	<b>0.3282</b>	<b>0.3693</b>
w/o Fusion	✗	✓	✓	✓	0.0860	0.0857
w/o CL	✓	✗	✓	✓	0.2983	0.3307
w/o Align	✓	✓	✗	✓	0.3231	0.3564
w/o Rec	✓	✓	✓	✗	0.2436	0.2586

#### 4.3.2 Impact of Sampling Rate

Table 3: Analysis of sampling rate optimization

$\rho$	Performance		Efficiency		
	Recall	NDCG	Time/epoch	Conv.	Total
1.0	0.3226	0.3567	75.30s	23	28.9m
0.1	0.3268	0.3604	68.03s	21	23.8m
0.01	<b>0.3282</b>	<b>0.3693</b>	59.57s	21	20.8m
0.001	0.2025	0.2050	50.01s	>50	>41.7m

Our sampling rate analysis empirically validates the theoretical bounds established in Theorem 3 through three critical regimes of operation. The full-graph training setting ( $\rho = 1.0$ ) corresponds to the  $C_1/t$ -dominated warm-up phase in our theoretical framework. While this configuration achieves reasonable performance (0.3226 Recall@20), it requires 28.9 minutes total training time, demonstrating the computational cost of unoptimized stability bounds. This setting serves as our baseline for comparison with sampling-optimized approaches.

The optimal sampling configuration ( $\rho = 0.01$ ) represents a critical balance point between the competing terms in our theoretical model. This rate effectively balances the  $C_2(\rho)/t$  term (where  $\kappa/\rho^2$  is bounded at  $10^4 \times \kappa$ ) and the  $\epsilon(\rho)/\sqrt{t}$  term from Theorem 3. The experimental results confirm that this configuration delivers the peak performance (0.3282 Recall@20) while requiring only 20.8 minutes of training, a 28.0% efficiency gain compared to full-graph training. This empirical finding aligns with the  $O(1/t)$  decay advantage predicted by our theoretical analysis.

### 4.4 Empirical Analysis

**Robustness Analysis** To evaluate the model robustness, we conduct experiments by randomly corrupting 0%-20% of user-item interactions. SDCGCL-DualFuse demonstrates the superior stability, maintaining 81.3% of its performance under 20% noise on MovieLens and 76.7% on Amazon. As shown in Figure 5, all SDCGCL variants exhibit improved robustness compared to their base counterparts, attributed to our dual-channel architecture and cross-channel calibration.

**Parameter Sensitivity** Our framework involves five key hyperparameters that control different aspects of model behavior. Through extensive analysis, we observe that moderate values consistently yield optimal performance: channel balancing parameter  $\alpha$  (0.1-0.4), contrastive learning parameter  $\beta$  (0.3-0.7), distribution alignment parameter  $\gamma$  (0.1-0.5), and negative feedback weight  $k$  (0.1-0.3). The auxiliary loss parameter  $\lambda$  shows stability in the range of 0.1-0.2. Figure 6 visualizes these effects across datasets. These findings confirm our theoretical analysis in Section 2.1.4, particularly regarding the necessity of distribution alignment.

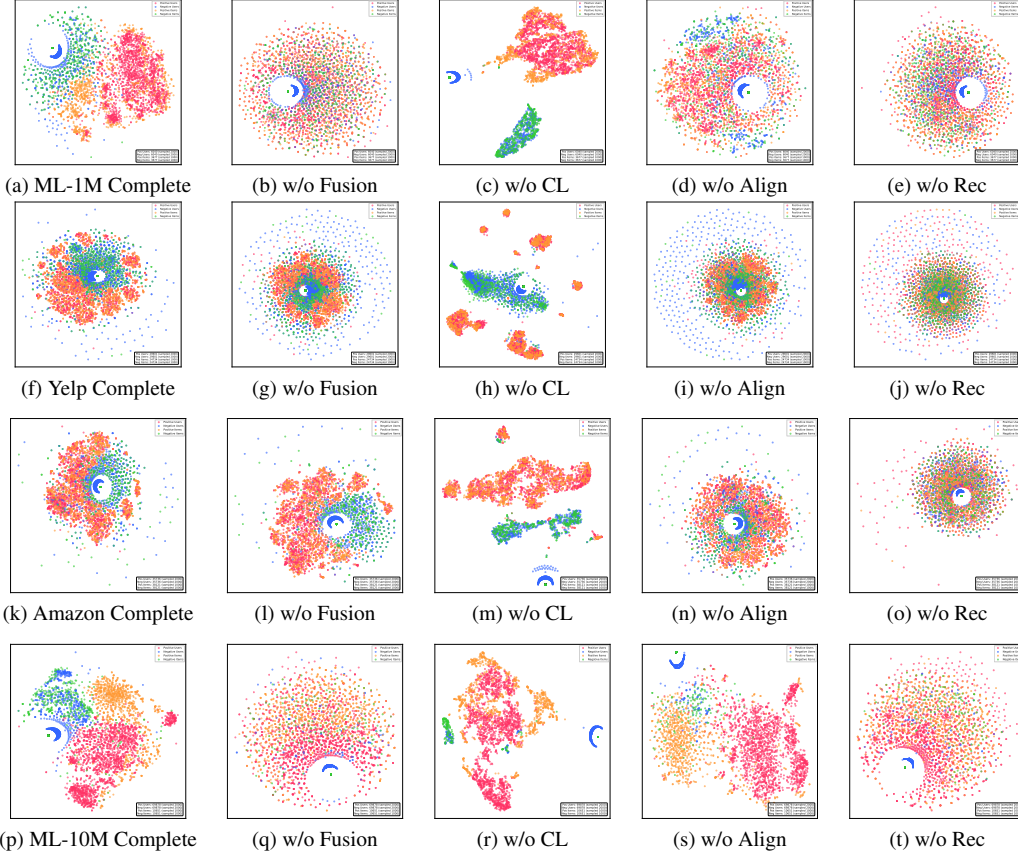


Figure 4: t-SNE visualization of learned embeddings on four datasets across different ablation settings. Red/orange: positive users/items; blue/green: negative users/items.

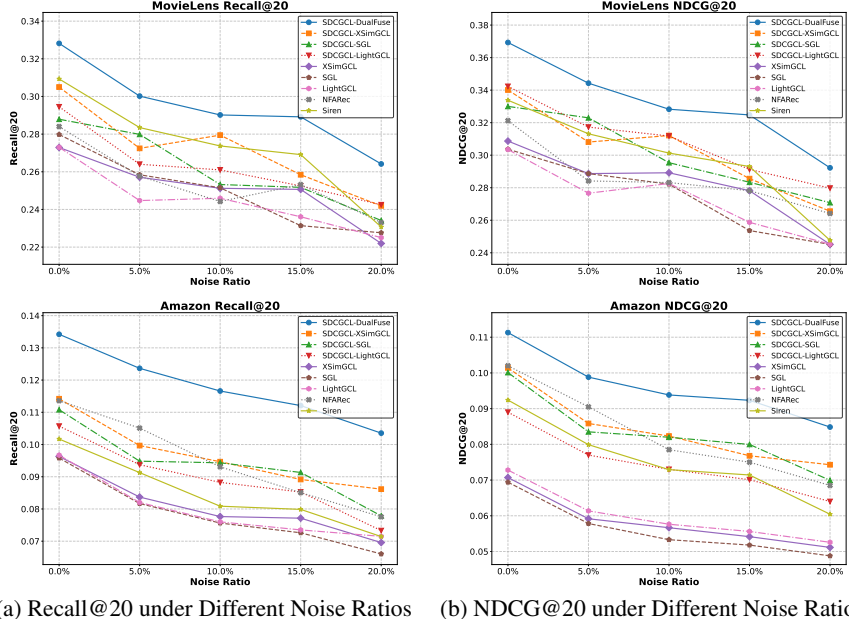


Figure 5: Model robustness evaluation on two datasets showing superior performance stability of SDCGCL variants under increasing noise ratios.

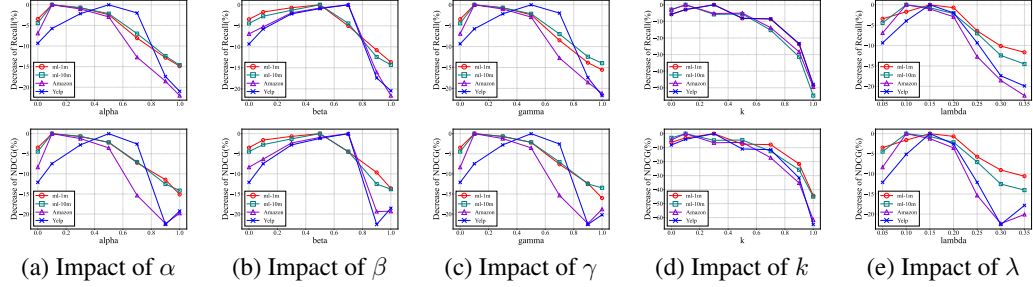


Figure 6: Parameter sensitivity analysis showing impact on Recall@20 and NDCG@20 across four datasets.

## 4.5 More Detailed Experiments

We provide additional experimental results in the appendix, including efficiency analysis (Appendix D.1), performance improvement analysis (Appendix D.2), and extended ablation studies (Appendix D.3) to supplement the main findings.

## 5 Related Work

### 5.1 GNNs for Recommendation

Deep learning[59, 37, 11, 26], especially GNN, has revolutionized recommender systems through their capacity to model complex user-item relationships. Starting with foundational works [33, 35], the field evolved through message passing innovations like GC-MC [36] and NGCF [40], reaching a significant milestone with LightGCN [16] and GCCF [5]. Subsequent developments enhanced theoretical foundations through pre-training [14], filtering mechanisms [58], and multi-view learning [61], while temporal modeling advanced through architectures like SRGNN [48], GCE-GNN [44], and TGSREC [10]. Dynamic patterns were captured by DGCF [41], TG-MC [1], DGSR [60], and SURGE [3], while contrastive learning emerged as a promising direction [2, 27, 57, 55, 53, 65, 64], further enhanced by transformer integrations [42, 51, 50]. However, these methods struggle with heterogeneous feedback types.

### 5.2 Sign-aware Recommendation

Sign-aware recommendation systems evolved from foundational explicit feedback methods like user-based CF [63], PMF [30], and SVD++ [23]. Built upon theoretical foundations in spectral analysis [18], matrix decomposition [19], and balance theory [17, 7], contemporary research has deepened understanding of negative feedback [22, 52], leading to innovations in graph-based systems [29, 34], sampling strategies [8, 9], interactive platforms [62], and sequential models [31, 32]. While various approaches have interpreted different user behaviors as negative signals [39, 12, 45, 62], many methods still struggle with effective integration, either excluding negative instances [54, 56] or oversimplifying interactions. Our work addresses these limitations through a model-agnostic framework that seamlessly integrates with existing methods while avoiding traditional balance theory constraints [34].

## 6 Conclusion

In this paper, we propose SDCGCL, a novel model-agnostic framework for effectively leveraging negative feedback in recommender systems, along with DualFuse, a specially designed model that maximizes the framework’s capabilities. Through theoretical analysis and extensive experiments, we demonstrate how our dual-channel architecture, cross-channel distribution calibration mechanism, and adaptive prediction strategy successfully address the fundamental challenges of incorporating negative feedback while maintaining computational efficiency. The framework’s model-agnostic nature enables seamless integration with existing graph contrastive learning methods, consistently yielding substantial performance improvements across multiple datasets and baseline models. Our comprehensive empirical results validate that negative feedback indeed plays a crucial role in enhancing recommendation performance when properly utilized through our proposed framework.

## Acknowledgments

This work is supported in part by the National Natural Science Foundation of China (No. 62372264 and No. 92467203) and Sina Weibo Corp. Chaokun Wang is the corresponding author.

## References

- [1] Esther Rodrigo Bonet, Duc Minh Nguyen, and Nikos Deligiannis. Temporal collaborative filtering with graph convolutional neural networks. In *2020 25th International Conference on Pattern Recognition (ICPR)*, pages 4736–4742. IEEE.
- [2] Xuheng Cai, Chao Huang, Lianghao Xia, and Xubin Ren. Lightgcl: Simple yet effective graph contrastive learning for recommendation. In *The Eleventh International Conference on Learning Representations*, 2023.
- [3] Jianxin Chang, Chen Gao, Yu Zheng, Yiqun Hui, Yanan Niu, Yang Song, Depeng Jin, and Yong Li. Sequential recommendation with graph neural networks. In *Proceedings of the 44th international ACM SIGIR conference on research and development in information retrieval*, pages 378–387, 2021.
- [4] Jinsong Chen, Gaichao Li, John E Hopcroft, and Kun He. Signgt: Signed attention-based graph transformer for graph representation learning. *arXiv preprint arXiv:2310.11025*, 2023.
- [5] Lei Chen, Le Wu, Richang Hong, Kun Zhang, and Meng Wang. Revisiting graph based collaborative filtering: A linear residual graph convolutional network approach. In *Proceedings of the AAAI conference on artificial intelligence*, volume 34, pages 27–34, 2020.
- [6] Sirui Chen, Jiawei Chen, Sheng Zhou, Bohao Wang, Shen Han, Chanfei Su, Yuqing Yuan, and Can Wang. Sigformer: Sign-aware graph transformer for recommendation. In *Proceedings of the 47th International ACM SIGIR Conference on Research and Development in Information Retrieval*, pages 1274–1284, 2024.
- [7] Tyler Derr, Yao Ma, and Jiliang Tang. Signed graph convolutional networks. In *2018 IEEE International Conference on Data Mining (ICDM)*, pages 929–934. IEEE, 2018.
- [8] Jingtao Ding, Fuli Feng, Xiangnan He, Guanghui Yu, Yong Li, and Depeng Jin. An improved sampler for bayesian personalized ranking by leveraging view data. In *Companion proceedings of the the web conference 2018*, pages 13–14, 2018.
- [9] Jingtao Ding, Yuhang Quan, Xiangnan He, Yong Li, and Depeng Jin. Reinforced negative sampling for recommendation with exposure data. In *IJCAI*, pages 2230–2236. Macao, 2019.
- [10] Ziwei Fan, Zhiwei Liu, Jiawei Zhang, Yun Xiong, Lei Zheng, and Philip S Yu. Continuous-time sequential recommendation with temporal graph collaborative transformer. In *Proceedings of the 30th ACM international conference on information & knowledge management*, pages 433–442, 2021.
- [11] Zhiyuan Feng, Zhaolu Kang, Qijie Wang, Zhiying Du, Jiongrui Yan, Shubin Shi, Chengbo Yuan, Huiyi Liang, Yu Deng, Qixiu Li, et al. Seeing across views: Benchmarking spatial reasoning of vision-language models in robotic scenes. *arXiv preprint arXiv:2510.19400*, 2025.
- [12] Shanshan Gong and Kenny Q Zhu. Positive, negative and neutral: Modeling implicit feedback in session-based news recommendation. In *Proceedings of the 45th international ACM SIGIR conference on research and development in information retrieval*, pages 1185–1195, 2022.
- [13] Zirui Guo, Yanhua Yu, Yuling Wang, Kangkang Lu, Zixuan Yang, Liang Pang, and Tat-Seng Chua. Information-controllable graph contrastive learning for recommendation. In *Proceedings of the 18th ACM Conference on Recommender Systems*, pages 528–537, 2024.
- [14] Bowen Hao, Jing Zhang, Hongzhi Yin, Cuiping Li, and Hong Chen. Pre-training graph neural networks for cold-start users and items representation. In *Proceedings of the 14th ACM International Conference on Web Search and Data Mining*, pages 265–273, 2021.

[15] Xiangnan He, Lizi Liao, Hanwang Zhang, Liqiang Nie, Xia Hu, and Tat-Seng Chua. Neural collaborative filtering. In *Proceedings of the 26th international conference on world wide web*, pages 173–182, 2017.

[16] Xiangnan He, Kuan Deng, Xiang Wang, Yan Li, Yongdong Zhang, and Meng Wang. Lightgen: Simplifying and powering graph convolution network for recommendation. In *Proceedings of the 43rd International ACM SIGIR conference on research and development in Information Retrieval*, pages 639–648, 2020.

[17] Fritz Heider. Attitudes and cognitive organization. *The Journal of psychology*, 21(1):107–112, 1946.

[18] Yaoping Hou, Jiongsheng Li, and Yongliang Pan. On the laplacian eigenvalues of signed graphs. *Linear and Multilinear Algebra*, 51(1):21–30, 2003.

[19] Cho-Jui Hsieh, Kai-Yang Chiang, and Inderjit S Dhillon. Low rank modeling of signed networks. In *Proceedings of the 18th ACM SIGKDD international conference on Knowledge discovery and data mining*, pages 507–515, 2012.

[20] Junjie Huang, Huawei Shen, Qi Cao, Shuchang Tao, and Xueqi Cheng. Signed bipartite graph neural networks. In *Proceedings of the 30th ACM international conference on information & knowledge management*, pages 740–749, 2021.

[21] Junjie Huang, Ruobing Xie, Qi Cao, Huawei Shen, Shaoliang Zhang, Feng Xia, and Xueqi Cheng. Negative can be positive: Signed graph neural networks for recommendation. *Information Processing & Management*, 60(4):103403, 2023.

[22] Olivier Jeunen. Revisiting offline evaluation for implicit-feedback recommender systems. In *Proceedings of the 13th ACM conference on recommender systems*, pages 596–600, 2019.

[23] Yehuda Koren, Robert Bell, and Chris Volinsky. Matrix factorization techniques for recommender systems. *Computer*, 42(8):30–37, 2009.

[24] Chaoliu Li, Lianghao Xia, Xubin Ren, Yaowen Ye, Yong Xu, and Chao Huang. Graph transformer for recommendation. In *Proceedings of the 46th International ACM SIGIR Conference on Research and Development in Information Retrieval*, pages 1680–1689, 2023.

[25] Yu Li, Meng Qu, Jian Tang, and Yi Chang. Signed laplacian graph neural networks. In *Proceedings of the AAAI conference on artificial intelligence*, volume 37, pages 4444–4452, 2023.

[26] Yuying Li, Siyi Qian, Hao Liang, Leqi Zheng, Ruichuan An, Yongzhen Guo, and Wentao Zhang. Capgeo: A caption-assisted approach to geometric reasoning. *arXiv preprint arXiv:2510.09302*, 2025.

[27] Zihan Lin, Changxin Tian, Yupeng Hou, and Wayne Xin Zhao. Improving graph collaborative filtering with neighborhood-enriched contrastive learning. In *Proceedings of the ACM web conference 2022*, pages 2320–2329, 2022.

[28] Yuxi Liu, Lianghao Xia, and Chao Huang. Selfgnn: Self-supervised graph neural networks for sequential recommendation. In *Proceedings of the 47th International ACM SIGIR Conference on Research and Development in Information Retrieval*, pages 1609–1618, 2024.

[29] Ziyang Liu, Chaokun Wang, Shuwen Zheng, Cheng Wu, Kai Zheng, Yang Song, and Na Mou. Pone-gnn: Integrating positive and negative feedback in graph neural networks for recommender systems. *ACM Trans. Recomm. Syst.*, 3(2), March 2025. doi: 10.1145/3711666. URL <https://doi.org/10.1145/3711666>.

[30] Andriy Mnih and Russ R Salakhutdinov. Probabilistic matrix factorization. *Advances in neural information processing systems*, 20, 2007.

[31] Yunzhu Pan, Chen Gao, Jianxin Chang, Yanan Niu, Yang Song, Kun Gai, Depeng Jin, and Yong Li. Understanding and modeling passive-negative feedback for short-video sequential recommendation. In *Proceedings of the 17th ACM conference on recommender systems*, pages 540–550, 2023.

[32] Minju Park and Kyogu Lee. Exploiting negative preference in content-based music recommendation with contrastive learning. In *Proceedings of the 16th ACM Conference on Recommender Systems*, pages 229–236, 2022.

[33] Nikhil Rao, Hsiang-Fu Yu, Pradeep K Ravikumar, and Inderjit S Dhillon. Collaborative filtering with graph information: Consistency and scalable methods. *Advances in neural information processing systems*, 28, 2015.

[34] Changwon Seo, Kyeong-Joong Jeong, Sungsu Lim, and Won-Yong Shin. Siren: Sign-aware recommendation using graph neural networks. *IEEE Transactions on Neural Networks and Learning Systems*, 35(4):4729–4743, 2022.

[35] Jiabin Tang, Yuhao Yang, Wei Wei, Lei Shi, Long Xia, Dawei Yin, and Chao Huang. Higpt: Heterogeneous graph language model. In *Proceedings of the 30th ACM SIGKDD Conference on Knowledge Discovery and Data Mining*, pages 2842–2853, 2024.

[36] Rianne van den Berg, Thomas N. Kipf, and Max Welling. Graph convolutional matrix completion. In *Proceedings of the 24th ACM SIGKDD International Conference on Knowledge Discovery & Data Mining (KDD)*, London, UK, 2018. Deep Learning Day.

[37] Jiahua Wang, Shannan Yan, Leqi Zheng, Jialong Wu, and Yaxin Mao. Audio-visual world models: Towards multisensory imagination in sight and sound. *arXiv preprint arXiv:2512.00883*, 2025.

[38] Jianling Wang, Kaize Ding, Liangjie Hong, Huan Liu, and James Caverlee. Next-item recommendation with sequential hypergraphs. In *Proceedings of the 43rd international ACM SIGIR conference on research and development in information retrieval*, pages 1101–1110, 2020.

[39] Wei Wang and Longbing Cao. Interactive sequential basket recommendation by learning basket couplings and positive/negative feedback. *ACM Transactions on Information Systems (TOIS)*, 39(3):1–26, 2021.

[40] Xiang Wang, Xiangnan He, Meng Wang, Fuli Feng, and Tat-Seng Chua. Neural graph collaborative filtering. In *Proceedings of the 42nd International ACM SIGIR Conference on Research and Development in Information Retrieval*, SIGIR’19, page 165–174, New York, NY, USA, 2019. Association for Computing Machinery. ISBN 9781450361729. doi: 10.1145/3331184.3331267.

[41] Xiang Wang, Hongye Jin, An Zhang, Xiangnan He, Tong Xu, and Tat-Seng Chua. Disentangled graph collaborative filtering. In *Proceedings of the 43rd international ACM SIGIR conference on research and development in information retrieval*, pages 1001–1010, 2020.

[42] Xinfeng Wang, Fumiyo Fukumoto, Jin Cui, Yoshimi Suzuki, Jiyi Li, and Dongjin Yu. Eedn: Enhanced encoder-decoder network with local and global context learning for poi recommendation. In *Proceedings of the 46th International ACM SIGIR Conference on Research and Development in Information Retrieval*, pages 383–392, 2023.

[43] Xinfeng Wang, Fumiyo Fukumoto, Jin Cui, Yoshimi Suzuki, and Dongjin Yu. Nfarec: A negative feedback-aware recommender model. In *Proceedings of the 47th International ACM SIGIR Conference on Research and Development in Information Retrieval*, pages 935–945, 2024.

[44] Ziyang Wang, Wei Wei, Gao Cong, Xiao-Li Li, Xian-Ling Mao, and Minghui Qiu. Global context enhanced graph neural networks for session-based recommendation. In *Proceedings of the 43rd international ACM SIGIR conference on research and development in information retrieval*, pages 169–178, 2020.

[45] Chuhan Wu, Fangzhao Wu, Yongfeng Huang, and Xing Xie. Neural news recommendation with negative feedback. *CCF Transactions on Pervasive Computing and Interaction*, 2:178–188, 2020.

[46] Jiancan Wu, Xiang Wang, Fuli Feng, Xiangnan He, Liang Chen, Jianxun Lian, and Xing Xie. Self-supervised graph learning for recommendation. In *Proceedings of the 44th international ACM SIGIR conference on research and development in information retrieval*, pages 726–735, 2021.

[47] Qitian Wu, Wentao Zhao, Chenxiao Yang, Hengrui Zhang, Fan Nie, Haitian Jiang, Yatao Bian, and Junchi Yan. Simplifying and empowering transformers for large-graph representations. *Advances in Neural Information Processing Systems*, 36, 2024.

[48] Shu Wu, Yuyuan Tang, Yanqiao Zhu, Liang Wang, Xing Xie, and Tieniu Tan. Session-based recommendation with graph neural networks. In *Proceedings of the AAAI conference on artificial intelligence*, volume 33, pages 346–353, 2019.

[49] Yiqing Wu, Ruobing Xie, Zhao Zhang, Xu Zhang, Fuzhen Zhuang, Leyu Lin, Zhanhui Kang, and Yongjun Xu. Dfgnn: Dual-frequency graph neural network for sign-aware feedback. In *Proceedings of the 30th ACM SIGKDD Conference on Knowledge Discovery and Data Mining*, pages 3437–3447, 2024.

[50] Lianghao Xia, Chao Huang, Yong Xu, Jiashu Zhao, Dawei Yin, and Jimmy Huang. Hypergraph contrastive collaborative filtering. In *Proceedings of the 45th International ACM SIGIR conference on research and development in information retrieval*, pages 70–79, 2022.

[51] Lianghao Xia, Chao Huang, and Chuxu Zhang. Self-supervised hypergraph transformer for recommender systems. In *Proceedings of the 28th ACM SIGKDD conference on knowledge discovery and data mining*, pages 2100–2109, 2022.

[52] Ruobing Xie, Cheng Ling, Yalong Wang, Rui Wang, Feng Xia, and Leyu Lin. Deep feedback network for recommendation. In *Proceedings of the twenty-ninth international conference on international joint conferences on artificial intelligence*, pages 2519–2525, 2021.

[53] Jingcao Xu, Chaokun Wang, Cheng Wu, Yang Song, Kai Zheng, Xiaowei Wang, Changping Wang, Guorui Zhou, and Kun Gai. Multi-behavior self-supervised learning for recommendation. In *Proceedings of the 46th international ACM SIGIR conference on research and development in information retrieval*, pages 496–505, 2023.

[54] Junliang Yu, Hongzhi Yin, Jundong Li, Min Gao, Zi Huang, and Lizhen Cui. Enhancing social recommendation with adversarial graph convolutional networks. *IEEE Transactions on knowledge and data engineering*, 34(8):3727–3739, 2020.

[55] Junliang Yu, Hongzhi Yin, Min Gao, Xin Xia, Xiangliang Zhang, and Nguyen Quoc Viet Hung. Socially-aware self-supervised tri-training for recommendation. In *Proceedings of the 27th ACM SIGKDD conference on knowledge discovery & data mining*, pages 2084–2092, 2021.

[56] Junliang Yu, Hongzhi Yin, Xin Xia, Tong Chen, Lizhen Cui, and Quoc Viet Hung Nguyen. Are graph augmentations necessary? simple graph contrastive learning for recommendation. In *Proceedings of the 45th international ACM SIGIR conference on research and development in information retrieval*, pages 1294–1303, 2022.

[57] Junliang Yu, Xin Xia, Tong Chen, Lizhen Cui, Nguyen Quoc Viet Hung, and Hongzhi Yin. Xsimgel: Towards extremely simple graph contrastive learning for recommendation. *IEEE Transactions on Knowledge and Data Engineering*, 36(2):913–926, 2023.

[58] Wenhui Yu, Zixin Zhang, and Zheng Qin. Low-pass graph convolutional network for recommendation. In *Proceedings of the AAAI Conference on Artificial Intelligence*, volume 36, pages 8954–8961, 2022.

[59] Hang Zhang, Chaokun Wang, Hongwei Li, Cheng Wu, Songyao Wang, Yabin Liu, Gengyuan Shi, and Ziyang Liu. Plforge: Enhancing language models for natural language to procedural extensions of sql. *Proc. ACM Manag. Data*, 3(6), December 2025. doi: 10.1145/3769813.

[60] Mengqi Zhang, Shu Wu, Xueli Yu, Qiang Liu, and Liang Wang. Dynamic graph neural networks for sequential recommendation. *IEEE Transactions on Knowledge and Data Engineering*, 35(5):4741–4753, 2022.

[61] Sen Zhao, Wei Wei, Ding Zou, and Xianling Mao. Multi-view intent disentangle graph networks for bundle recommendation. In *Proceedings of the AAAI Conference on Artificial Intelligence*, volume 36, pages 4379–4387, 2022.

[62] Xiangyu Zhao, Liang Zhang, Zhuoye Ding, Long Xia, Jiliang Tang, and Dawei Yin. Recommendations with negative feedback via pairwise deep reinforcement learning. In *Proceedings of the 24th ACM SIGKDD international conference on knowledge discovery & data mining*, pages 1040–1048, 2018.

[63] Zhi-Dan Zhao and Ming-Sheng Shang. User-based collaborative-filtering recommendation algorithms on hadoop. In *2010 third international conference on knowledge discovery and data mining*, pages 478–481. IEEE, 2010.

[64] Leqi Zheng, Chaokun Wang, Canzhi Chen, Jiajun Zhang, Cheng Wu, Zixin Song, Shannan Yan, Ziyang Liu, and Hongwei Li. LAGCL4Rec: When LLMs activate interactions potential in graph contrastive learning for recommendation. In *Findings of the Association for Computational Linguistics: EMNLP 2025*, pages 1163–1184, Suzhou, China, November 2025. Association for Computational Linguistics. doi: 10.18653/v1/2025.findings-emnlp.61.

[65] Leqi Zheng, Chaokun Wang, Ziyang Liu, Canzhi Chen, Cheng Wu, and Hongwei Li. Balancing self-presentation and self-hiding for exposure-aware recommendation based on graph contrastive learning. In *Proceedings of the 48th International ACM SIGIR Conference on Research and Development in Information Retrieval*, pages 2027–2037, 2025.

## NeurIPS Paper Checklist

### 1. Claims

Question: Do the main claims made in the abstract and introduction accurately reflect the paper's contributions and scope?

Answer: [\[Yes\]](#)

Justification: The abstract and introduction clearly state the contributions of proposing SDCGCL framework, addressing model compatibility, information exchange, and computational efficiency challenges. Key claims align with theoretical analysis and experimental results in Sections 2, 3, 4.

Guidelines:

- The answer NA means that the abstract and introduction do not include the claims made in the paper.
- The abstract and/or introduction should clearly state the claims made, including the contributions made in the paper and important assumptions and limitations. A No or NA answer to this question will not be perceived well by the reviewers.
- The claims made should match theoretical and experimental results, and reflect how much the results can be expected to generalize to other settings.
- It is fine to include aspirational goals as motivation as long as it is clear that these goals are not attained by the paper.

### 2. Limitations

Question: Does the paper discuss the limitations of the work performed by the authors?

Answer: [\[Yes\]](#)

Justification: Limitations are discussed in Appendix E, including scalability to industrial systems, dynamic feedback modeling, and cold-start scenarios.

Guidelines:

- The answer NA means that the paper has no limitation while the answer No means that the paper has limitations, but those are not discussed in the paper.
- The authors are encouraged to create a separate "Limitations" section in their paper.
- The paper should point out any strong assumptions and how robust the results are to violations of these assumptions (e.g., independence assumptions, noiseless settings, model well-specification, asymptotic approximations only holding locally). The authors should reflect on how these assumptions might be violated in practice and what the implications would be.

- The authors should reflect on the scope of the claims made, e.g., if the approach was only tested on a few datasets or with a few runs. In general, empirical results often depend on implicit assumptions, which should be articulated.
- The authors should reflect on the factors that influence the performance of the approach. For example, a facial recognition algorithm may perform poorly when image resolution is low or images are taken in low lighting. Or a speech-to-text system might not be used reliably to provide closed captions for online lectures because it fails to handle technical jargon.
- The authors should discuss the computational efficiency of the proposed algorithms and how they scale with dataset size.
- If applicable, the authors should discuss possible limitations of their approach to address problems of privacy and fairness.
- While the authors might fear that complete honesty about limitations might be used by reviewers as grounds for rejection, a worse outcome might be that reviewers discover limitations that aren't acknowledged in the paper. The authors should use their best judgment and recognize that individual actions in favor of transparency play an important role in developing norms that preserve the integrity of the community. Reviewers will be specifically instructed to not penalize honesty concerning limitations.

### 3. Theory assumptions and proofs

Question: For each theoretical result, does the paper provide the full set of assumptions and a complete (and correct) proof?

Answer: [\[Yes\]](#)

Justification: Assumptions and Complete proofs (e.g., negative feedback instability, gradient balance) are explicitly stated in Section 2.1.4, 2.2.3, 3.1 and Appendix A.1, A.2, A.3.

Guidelines:

- The answer NA means that the paper does not include theoretical results.
- All the theorems, formulas, and proofs in the paper should be numbered and cross-referenced.
- All assumptions should be clearly stated or referenced in the statement of any theorems.
- The proofs can either appear in the main paper or the supplemental material, but if they appear in the supplemental material, the authors are encouraged to provide a short proof sketch to provide intuition.
- Inversely, any informal proof provided in the core of the paper should be complemented by formal proofs provided in appendix or supplemental material.
- Theorems and Lemmas that the proof relies upon should be properly referenced.

### 4. Experimental result reproducibility

Question: Does the paper fully disclose all the information needed to reproduce the main experimental results of the paper to the extent that it affects the main claims and/or conclusions of the paper (regardless of whether the code and data are provided or not)?

Answer: [\[Yes\]](#)

Justification: The paper uses four public datasets (ML-1M, Yelp, Amazon, ML-10M) with standardized preprocessing (Appendix C). Implementation details (hyperparameters, architectures) are provided in Sections 2, 3 and Appendix C.

Guidelines:

- The answer NA means that the paper does not include experiments.
- If the paper includes experiments, a No answer to this question will not be perceived well by the reviewers: Making the paper reproducible is important, regardless of whether the code and data are provided or not.
- If the contribution is a dataset and/or model, the authors should describe the steps taken to make their results reproducible or verifiable.
- Depending on the contribution, reproducibility can be accomplished in various ways. For example, if the contribution is a novel architecture, describing the architecture fully might suffice, or if the contribution is a specific model and empirical evaluation, it may

be necessary to either make it possible for others to replicate the model with the same dataset, or provide access to the model. In general, releasing code and data is often one good way to accomplish this, but reproducibility can also be provided via detailed instructions for how to replicate the results, access to a hosted model (e.g., in the case of a large language model), releasing of a model checkpoint, or other means that are appropriate to the research performed.

- While NeurIPS does not require releasing code, the conference does require all submissions to provide some reasonable avenue for reproducibility, which may depend on the nature of the contribution. For example
  - (a) If the contribution is primarily a new algorithm, the paper should make it clear how to reproduce that algorithm.
  - (b) If the contribution is primarily a new model architecture, the paper should describe the architecture clearly and fully.
  - (c) If the contribution is a new model (e.g., a large language model), then there should either be a way to access this model for reproducing the results or a way to reproduce the model (e.g., with an open-source dataset or instructions for how to construct the dataset).
  - (d) We recognize that reproducibility may be tricky in some cases, in which case authors are welcome to describe the particular way they provide for reproducibility. In the case of closed-source models, it may be that access to the model is limited in some way (e.g., to registered users), but it should be possible for other researchers to have some path to reproducing or verifying the results.

## 5. Open access to data and code

Question: Does the paper provide open access to the data and code, with sufficient instructions to faithfully reproduce the main experimental results, as described in supplemental material?

Answer: [\[Yes\]](#)

Justification: We provide our data and code in the github.

Guidelines:

- The answer NA means that paper does not include experiments requiring code.
- Please see the NeurIPS code and data submission guidelines (<https://nips.cc/public/guides/CodeSubmissionPolicy>) for more details.
- While we encourage the release of code and data, we understand that this might not be possible, so “No” is an acceptable answer. Papers cannot be rejected simply for not including code, unless this is central to the contribution (e.g., for a new open-source benchmark).
- The instructions should contain the exact command and environment needed to run to reproduce the results. See the NeurIPS code and data submission guidelines (<https://nips.cc/public/guides/CodeSubmissionPolicy>) for more details.
- The authors should provide instructions on data access and preparation, including how to access the raw data, preprocessed data, intermediate data, and generated data, etc.
- The authors should provide scripts to reproduce all experimental results for the new proposed method and baselines. If only a subset of experiments are reproducible, they should state which ones are omitted from the script and why.
- At submission time, to preserve anonymity, the authors should release anonymized versions (if applicable).
- Providing as much information as possible in supplemental material (appended to the paper) is recommended, but including URLs to data and code is permitted.

## 6. Experimental setting/details

Question: Does the paper specify all the training and test details (e.g., data splits, hyperparameters, how they were chosen, type of optimizer, etc.) necessary to understand the results?

Answer: [\[Yes\]](#)

Justification: Implementation details (hyperparameters, architectures) are provided in Sections 2, 3 and Appendix C.

Guidelines:

- The answer NA means that the paper does not include experiments.
- The experimental setting should be presented in the core of the paper to a level of detail that is necessary to appreciate the results and make sense of them.
- The full details can be provided either with the code, in appendix, or as supplemental material.

## 7. Experiment statistical significance

Question: Does the paper report error bars suitably and correctly defined or other appropriate information about the statistical significance of the experiments?

Answer: **[Yes]**

Justification: Statistical significance ( $p < 0.01$ ) is reported in Table 1.

Guidelines:

- The answer NA means that the paper does not include experiments.
- The authors should answer "Yes" if the results are accompanied by error bars, confidence intervals, or statistical significance tests, at least for the experiments that support the main claims of the paper.
- The factors of variability that the error bars are capturing should be clearly stated (for example, train/test split, initialization, random drawing of some parameter, or overall run with given experimental conditions).
- The method for calculating the error bars should be explained (closed form formula, call to a library function, bootstrap, etc.)
- The assumptions made should be given (e.g., Normally distributed errors).
- It should be clear whether the error bar is the standard deviation or the standard error of the mean.
- It is OK to report 1-sigma error bars, but one should state it. The authors should preferably report a 2-sigma error bar than state that they have a 96% CI, if the hypothesis of Normality of errors is not verified.
- For asymmetric distributions, the authors should be careful not to show in tables or figures symmetric error bars that would yield results that are out of range (e.g. negative error rates).
- If error bars are reported in tables or plots, The authors should explain in the text how they were calculated and reference the corresponding figures or tables in the text.

## 8. Experiments compute resources

Question: For each experiment, does the paper provide sufficient information on the computer resources (type of compute workers, memory, time of execution) needed to reproduce the experiments?

Answer: **[Yes]**

Justification: Hardware specifications (8xRTX3090 GPUs) and training times per epoch are provided in Appendix D.1. Total training times are reported in Table 5.

Guidelines:

- The answer NA means that the paper does not include experiments.
- The paper should indicate the type of compute workers CPU or GPU, internal cluster, or cloud provider, including relevant memory and storage.
- The paper should provide the amount of compute required for each of the individual experimental runs as well as estimate the total compute.
- The paper should disclose whether the full research project required more compute than the experiments reported in the paper (e.g., preliminary or failed experiments that didn't make it into the paper).

## 9. Code of ethics

Question: Does the research conducted in the paper conform, in every respect, with the NeurIPS Code of Ethics <https://neurips.cc/public/EthicsGuidelines>?

Answer: [\[Yes\]](#)

Justification: The work complies with NeurIPS ethics guidelines. No human subjects, biased data, or high-risk applications are involved. Focus is on algorithmic improvements for recommendation systems.

Guidelines:

- The answer NA means that the authors have not reviewed the NeurIPS Code of Ethics.
- If the authors answer No, they should explain the special circumstances that require a deviation from the Code of Ethics.
- The authors should make sure to preserve anonymity (e.g., if there is a special consideration due to laws or regulations in their jurisdiction).

## 10. Broader impacts

Question: Does the paper discuss both potential positive societal impacts and negative societal impacts of the work performed?

Answer: [\[Yes\]](#)

Justification: The recommendation algorithm has a positive impact on the field of recommender systems. The impact is discussed in Section F.

Guidelines:

- The answer NA means that there is no societal impact of the work performed.
- If the authors answer NA or No, they should explain why their work has no societal impact or why the paper does not address societal impact.
- Examples of negative societal impacts include potential malicious or unintended uses (e.g., disinformation, generating fake profiles, surveillance), fairness considerations (e.g., deployment of technologies that could make decisions that unfairly impact specific groups), privacy considerations, and security considerations.
- The conference expects that many papers will be foundational research and not tied to particular applications, let alone deployments. However, if there is a direct path to any negative applications, the authors should point it out. For example, it is legitimate to point out that an improvement in the quality of generative models could be used to generate deepfakes for disinformation. On the other hand, it is not needed to point out that a generic algorithm for optimizing neural networks could enable people to train models that generate Deepfakes faster.
- The authors should consider possible harms that could arise when the technology is being used as intended and functioning correctly, harms that could arise when the technology is being used as intended but gives incorrect results, and harms following from (intentional or unintentional) misuse of the technology.
- If there are negative societal impacts, the authors could also discuss possible mitigation strategies (e.g., gated release of models, providing defenses in addition to attacks, mechanisms for monitoring misuse, mechanisms to monitor how a system learns from feedback over time, improving the efficiency and accessibility of ML).

## 11. Safeguards

Question: Does the paper describe safeguards that have been put in place for responsible release of data or models that have a high risk for misuse (e.g., pretrained language models, image generators, or scraped datasets)?

Answer: [\[NA\]](#)

Justification: The work does not involve high-risk models or sensitive data. SDCGCL is a recommendation framework evaluated on public rating datasets.

Guidelines:

- The answer NA means that the paper poses no such risks.

- Released models that have a high risk for misuse or dual-use should be released with necessary safeguards to allow for controlled use of the model, for example by requiring that users adhere to usage guidelines or restrictions to access the model or implementing safety filters.
- Datasets that have been scraped from the Internet could pose safety risks. The authors should describe how they avoided releasing unsafe images.
- We recognize that providing effective safeguards is challenging, and many papers do not require this, but we encourage authors to take this into account and make a best faith effort.

## 12. Licenses for existing assets

Question: Are the creators or original owners of assets (e.g., code, data, models), used in the paper, properly credited and are the license and terms of use explicitly mentioned and properly respected?

Answer: **[Yes]**

Justification: Public datasets (ML-1M, Yelp, Amazon) are cited in Appendix C.

Guidelines:

- The answer NA means that the paper does not use existing assets.
- The authors should cite the original paper that produced the code package or dataset.
- The authors should state which version of the asset is used and, if possible, include a URL.
- The name of the license (e.g., CC-BY 4.0) should be included for each asset.
- For scraped data from a particular source (e.g., website), the copyright and terms of service of that source should be provided.
- If assets are released, the license, copyright information, and terms of use in the package should be provided. For popular datasets, [paperswithcode.com/datasets](http://paperswithcode.com/datasets) has curated licenses for some datasets. Their licensing guide can help determine the license of a dataset.
- For existing datasets that are re-packaged, both the original license and the license of the derived asset (if it has changed) should be provided.
- If this information is not available online, the authors are encouraged to reach out to the asset's creators.

## 13. New assets

Question: Are new assets introduced in the paper well documented and is the documentation provided alongside the assets?

Answer: **[Yes]**

Justification: Code and model checkpoints are released with documentation. Anonymization is maintained for submission

Guidelines:

- The answer NA means that the paper does not release new assets.
- Researchers should communicate the details of the dataset/code/model as part of their submissions via structured templates. This includes details about training, license, limitations, etc.
- The paper should discuss whether and how consent was obtained from people whose asset is used.
- At submission time, remember to anonymize your assets (if applicable). You can either create an anonymized URL or include an anonymized zip file.

## 14. Crowdsourcing and research with human subjects

Question: For crowdsourcing experiments and research with human subjects, does the paper include the full text of instructions given to participants and screenshots, if applicable, as well as details about compensation (if any)?

Answer: **[NA]**

Justification: No human subject research or crowdsourcing is involved. Experiments use pre-collected public interaction data.

Guidelines:

- The answer NA means that the paper does not involve crowdsourcing nor research with human subjects.
- Including this information in the supplemental material is fine, but if the main contribution of the paper involves human subjects, then as much detail as possible should be included in the main paper.
- According to the NeurIPS Code of Ethics, workers involved in data collection, curation, or other labor should be paid at least the minimum wage in the country of the data collector.

#### 15. Institutional review board (IRB) approvals or equivalent for research with human subjects

Question: Does the paper describe potential risks incurred by study participants, whether such risks were disclosed to the subjects, and whether Institutional Review Board (IRB) approvals (or an equivalent approval/review based on the requirements of your country or institution) were obtained?

Answer: [NA]

Justification: Not applicable, as no human subjects were involved.

Guidelines:

- The answer NA means that the paper does not involve crowdsourcing nor research with human subjects.
- Depending on the country in which research is conducted, IRB approval (or equivalent) may be required for any human subjects research. If you obtained IRB approval, you should clearly state this in the paper.
- We recognize that the procedures for this may vary significantly between institutions and locations, and we expect authors to adhere to the NeurIPS Code of Ethics and the guidelines for their institution.
- For initial submissions, do not include any information that would break anonymity (if applicable), such as the institution conducting the review.

#### 16. Declaration of LLM usage

Question: Does the paper describe the usage of LLMs if it is an important, original, or non-standard component of the core methods in this research? Note that if the LLM is used only for writing, editing, or formatting purposes and does not impact the core methodology, scientific rigorousness, or originality of the research, declaration is not required.

Answer: [NA]

Justification: LLMs are not used in methodology or experiments. The work focuses on graph-based recommendation systems.

Guidelines:

- The answer NA means that the core method development in this research does not involve LLMs as any important, original, or non-standard components.
- Please refer to our LLM policy (<https://neurips.cc/Conferences/2025/LLM>) for what should or should not be described.

## A Detailed Proofs

### A.1 Complete Proof of Theorem 2.1: Distribution Instability

*Proof.* We begin by establishing the distributional properties of embeddings derived from positive and negative feedback channels. Given the assumptions stated in the theorem, we proceed as follows:

Let us denote  $X_{ui}^+ = \mathbf{E}_u^+ \circ \mathbf{E}_i^{+\top}$  and  $X_{ui}^- = \mathbf{E}_u^- \circ \mathbf{E}_i^{-\top}$  as the interaction scores in positive and negative channels, respectively. By assumption, these random variables follow distributions with

$$\begin{aligned}\mathbb{E}[X_{ui}^+] &= \mu, & \text{Var}[X_{ui}^+] &= \sigma^2 \\ \mathbb{E}[X_{ui}^-] &= \mu + \delta_1, & \text{Var}[X_{ui}^-] &= \delta_2 \sigma^2\end{aligned}\tag{15}$$

where  $\delta_1$  represents the mean shift and  $\delta_2 \geq 1$  captures the increased variance in negative feedback distributions.

For the predicted preference score  $\hat{y}_{u,i} = (1+k)X_{ui}^+ - kX_{ui}^-$ , we derive its expectation:

$$\begin{aligned}\mathbb{E}[\hat{y}_{u,i}] &= \mathbb{E}[(1+k)X_{ui}^+ - kX_{ui}^-] \\ &= (1+k)\mathbb{E}[X_{ui}^+] - k\mathbb{E}[X_{ui}^-] \\ &= (1+k)\mu - k(\mu + \delta_1) \\ &= (1+k)\mu - k\mu - k\delta_1 \\ &= \mu - k\delta_1\end{aligned}\tag{16}$$

Assuming independence between channels, we derive the variance:

$$\begin{aligned}\text{Var}[\hat{y}_{u,i}] &= \text{Var}[(1+k)X_{ui}^+ - kX_{ui}^-] \\ &= (1+k)^2 \text{Var}[X_{ui}^+] + k^2 \text{Var}[X_{ui}^-] \\ &= (1+k)^2 \sigma^2 + k^2 \delta_2 \sigma^2 \\ &= \sigma^2[(1+k)^2 + k^2 \delta_2] \\ &= \sigma^2[1 + 2k + k^2 + k^2 \delta_2] \\ &= \sigma^2[1 + 2k + k^2(1 + \delta_2)]\end{aligned}\tag{17}$$

This demonstrates that without distribution alignment, the prediction has a systematic bias of  $-k\delta_1$  and inflated variance scaled by  $\delta_2 \geq 1$ .

When applying our cross-channel distribution calibration mechanism (Equation 7), we enforce  $\delta_1 \rightarrow 0$  and  $\delta_2 \rightarrow 1$ . Consequently:

$$\begin{aligned}\mathbb{E}[\hat{y}_{u,i}] &= \mu \\ \text{Var}[\hat{y}_{u,i}] &= \sigma^2[1 + 2k + k^2(1 + 1)] \\ &= \sigma^2(1 + 2k + 2k^2)\end{aligned}\tag{18}$$

Thus, the alignment mechanism eliminates the bias term  $-k\delta_1$  from the prediction expectation and normalizes the variance to a more stable form that depends solely on  $k$  rather than the instability parameter  $\delta_2$ , completing the proof.  $\square$

## A.2 Complete Proof of Theorem 2.2: Cross-Channel Information Preservation

*Proof.* We analyze the gradient flow through the cross-channel fusion mechanism to demonstrate that it maintains balanced information flow between positive and negative channels.

### 1. Gradient Analysis for Positive Channel:

For the positive channel fusion operation, the gradient with respect to the embedding  $\mathbf{e}_v^+$  can be expressed as:

$$\begin{aligned}\nabla_{\mathbf{e}_v^+} \mathcal{L} &= \frac{\partial \mathcal{L}}{\partial \mathbf{e}_v^+} \\ &= \frac{\partial \mathcal{L}}{\partial \mathbf{Z}_v^+} \frac{\partial \mathbf{Z}_v^+}{\partial \mathbf{e}_v^+} + \frac{\partial \mathcal{L}}{\partial \mathbf{Z}_v^-} \frac{\partial \mathbf{Z}_v^-}{\partial \mathbf{e}_v^+}\end{aligned}\tag{19}$$

The first term corresponds to the direct gradient flow within the positive channel, while the second term captures the cross-channel influence through the fusion mechanism.

From Equation 13 in the main paper, we have:

$$\begin{aligned}\mathbf{Z}_v^+ &= \frac{1}{L+1} \sum_{l=0}^L \left( \mathbf{e}_{v,l^*}^+ + \frac{\mathbf{e}_{v,l^*}^-}{\|\mathbf{e}_{v,l^*}^-\|} \right) \\ \mathbf{Z}_v^- &= \frac{1}{L+1} \sum_{l=0}^L \left( \mathbf{e}_{v,l^*}^- + \frac{\mathbf{e}_{v,l^*}^+}{\|\mathbf{e}_{v,l^*}^+\|} \right)\end{aligned}\tag{20}$$

Therefore:

$$\begin{aligned}\frac{\partial \mathbf{Z}_v^+}{\partial \mathbf{e}_v^+} &= \frac{1}{L+1} \\ \frac{\partial \mathbf{Z}_v^-}{\partial \mathbf{e}_v^+} &= \frac{1}{L+1} \frac{\partial}{\partial \mathbf{e}_v^+} \left( \frac{\mathbf{e}_v^+}{\|\mathbf{e}_v^+\|} \right)\end{aligned}\tag{21}$$

The derivative of the normalized vector can be expanded as:

$$\begin{aligned}\frac{\partial}{\partial \mathbf{e}_v^+} \left( \frac{\mathbf{e}_v^+}{\|\mathbf{e}_v^+\|} \right) &= \frac{\partial}{\partial \mathbf{e}_v^+} \left( \frac{\mathbf{e}_v^+}{\sqrt{\mathbf{e}_v^+ \cdot \mathbf{e}_v^+}} \right) \\ &= \frac{1}{\|\mathbf{e}_v^+\|} \mathbf{I} - \frac{\mathbf{e}_v^+ \mathbf{e}_v^{+T}}{\|\mathbf{e}_v^+\|^3}\end{aligned}\tag{22}$$

where  $\mathbf{I}$  is the identity matrix.

For simplicity and to understand the upper bound, we can establish:

$$\left\| \frac{\partial}{\partial \mathbf{e}_v^+} \left( \frac{\mathbf{e}_v^+}{\|\mathbf{e}_v^+\|} \right) \right\| \leq \frac{1}{\|\mathbf{e}_v^+\|}\tag{23}$$

## 2. Gradient Norm Bounds:

Using the above results, we can now bound the gradient norm:

$$\begin{aligned}\|\nabla_{\mathbf{e}_v^+} \mathcal{L}\| &= \left\| \frac{\partial \mathcal{L}}{\partial \mathbf{Z}_v^+} \frac{\partial \mathbf{Z}_v^+}{\partial \mathbf{e}_v^+} + \frac{\partial \mathcal{L}}{\partial \mathbf{Z}_v^-} \frac{\partial \mathbf{Z}_v^-}{\partial \mathbf{e}_v^+} \right\| \\ &\leq \left\| \frac{\partial \mathcal{L}}{\partial \mathbf{Z}_v^+} \frac{\partial \mathbf{Z}_v^+}{\partial \mathbf{e}_v^+} \right\| + \left\| \frac{\partial \mathcal{L}}{\partial \mathbf{Z}_v^-} \frac{\partial \mathbf{Z}_v^-}{\partial \mathbf{e}_v^+} \right\| \\ &\leq \left\| \frac{\partial \mathcal{L}}{\partial \mathbf{Z}_v^+} \right\| \frac{1}{L+1} + \left\| \frac{\partial \mathcal{L}}{\partial \mathbf{Z}_v^-} \right\| \frac{1}{L+1} \frac{1}{\|\mathbf{e}_v^+\|} \\ &= \frac{1}{L+1} \left( \left\| \frac{\partial \mathcal{L}}{\partial \mathbf{Z}_v^+} \right\| + \left\| \frac{\partial \mathcal{L}}{\partial \mathbf{Z}_v^-} \right\| \frac{1}{\|\mathbf{e}_v^+\|} \right)\end{aligned}\tag{24}$$

Similarly, for the negative channel:

$$\|\nabla_{\mathbf{e}_v^-} \mathcal{L}\| \leq \frac{1}{L+1} \left( \left\| \frac{\partial \mathcal{L}}{\partial \mathbf{Z}_v^-} \right\| + \left\| \frac{\partial \mathcal{L}}{\partial \mathbf{Z}_v^+} \right\| \frac{1}{\|\mathbf{e}_v^-\|} \right)\tag{25}$$

## 3. Establishing Lower Bounds:

We can also establish lower bounds:

$$\begin{aligned}\|\nabla_{\mathbf{e}_v^+} \mathcal{L}\| &\geq \frac{1}{L+1} \left( \left\| \frac{\partial \mathcal{L}}{\partial \mathbf{Z}_v^+} \right\| - \left\| \frac{\partial \mathcal{L}}{\partial \mathbf{Z}_v^-} \right\| \frac{1}{\|\mathbf{e}_v^+\|} \right) \\ \|\nabla_{\mathbf{e}_v^-} \mathcal{L}\| &\geq \frac{1}{L+1} \left( \left\| \frac{\partial \mathcal{L}}{\partial \mathbf{Z}_v^-} \right\| - \left\| \frac{\partial \mathcal{L}}{\partial \mathbf{Z}_v^+} \right\| \frac{1}{\|\mathbf{e}_v^-\|} \right)\end{aligned}\tag{26}$$

#### 4. Convergence Analysis:

At convergence, several key conditions are satisfied:

- 1) The loss gradients with respect to contrastive embeddings from both channels become approximately equal:  $\left\| \frac{\partial \mathcal{L}}{\partial \mathbf{Z}_v^+} \right\| \approx \left\| \frac{\partial \mathcal{L}}{\partial \mathbf{Z}_v^-} \right\|$ .
- 2) The embedding norms from both channels converge to similar magnitudes:  $\|\mathbf{e}_v^+\| \approx \|\mathbf{e}_v^-\|$ .

Substituting these conditions into our bounds:

$$\begin{aligned}\frac{1}{L+1} \left( 1 - \frac{1}{\|\mathbf{e}_v^+\|} \right) \left\| \frac{\partial \mathcal{L}}{\partial \mathbf{Z}_v^+} \right\| &\leq \|\nabla_{\mathbf{e}_v^+} \mathcal{L}\| \leq \frac{1}{L+1} \left( 1 + \frac{1}{\|\mathbf{e}_v^+\|} \right) \left\| \frac{\partial \mathcal{L}}{\partial \mathbf{Z}_v^+} \right\| \\ \frac{1}{L+1} \left( 1 - \frac{1}{\|\mathbf{e}_v^-\|} \right) \left\| \frac{\partial \mathcal{L}}{\partial \mathbf{Z}_v^-} \right\| &\leq \|\nabla_{\mathbf{e}_v^-} \mathcal{L}\| \leq \frac{1}{L+1} \left( 1 + \frac{1}{\|\mathbf{e}_v^-\|} \right) \left\| \frac{\partial \mathcal{L}}{\partial \mathbf{Z}_v^-} \right\|\end{aligned}\tag{27}$$

Since  $\left\| \frac{\partial \mathcal{L}}{\partial \mathbf{Z}_v^+} \right\| \approx \left\| \frac{\partial \mathcal{L}}{\partial \mathbf{Z}_v^-} \right\|$  and  $\|\mathbf{e}_v^+\| \approx \|\mathbf{e}_v^-\|$  at convergence, we can conclude that:

$$\|\nabla_{\mathbf{e}_v^+} \mathcal{L}\| \approx \|\nabla_{\mathbf{e}_v^-} \mathcal{L}\|\tag{28}$$

This demonstrates that our cross-channel fusion mechanism maintains balanced gradient flow between positive and negative channels, ensuring that both channels contribute roughly equally to the learning process despite their potentially different initial characteristics.  $\square$

#### A.3 Complete Proof of Theorem 3.1: Two-Stage Stability Bound

*Proof.* We'll analyze each stage of our optimization process separately.

##### 1. Warmup Stage Analysis (Full-Graph Learning):

During the warmup stage ( $t \leq T_{\text{warm}}$ ), we train on the complete graph without sampling. Under standard assumptions for gradient-based optimization, the loss function  $\mathcal{L}$  has  $L$ -Lipschitz gradients in dense interaction regions where  $\|\mathbf{e}_u - \mathbf{e}_i\|_2 \geq \delta$ , the maximum distance between any node embeddings is bounded by  $D$  and the learning rate is initialized as  $\eta_0$  and potentially follows a schedule.

For gradient descent with these conditions, we have:

$$\begin{aligned}\mathbf{e}_v^{(t)} - \mathbf{e}_v^{(t-1)} &= -\eta_{t-1} \nabla_{\mathbf{e}_v} \mathcal{L}(\Theta^{(t-1)}) \\ \|\mathbf{e}_v^{(t)} - \mathbf{e}_v^{(t-1)}\|_2^2 &= \eta_{t-1}^2 \|\nabla_{\mathbf{e}_v} \mathcal{L}(\Theta^{(t-1)})\|_2^2\end{aligned}\tag{29}$$

By the Lipschitz gradient assumption in dense regions:

$$\|\nabla_{\mathbf{e}_v} \mathcal{L}(\Theta^{(t-1)})\|_2^2 \leq L^2 D\tag{30}$$

With learning rate schedule  $\eta_t = \eta_0 / \sqrt{t+1}$ , we get:

$$\begin{aligned}\mathbb{E} \|\mathbf{e}_v^{(t)} - \mathbf{e}_v^{(t-1)}\|_2^2 &\leq \eta_{t-1}^2 L^2 D \\ &= \frac{\eta_0^2}{t} L^2 D \\ &= \frac{C_1}{t}\end{aligned}\tag{31}$$

where  $C_1 = \eta_0^2 L^2 D$  is our warmup stage constant.

## 2. Sampling Stage Analysis (Subgraph Learning):

After the warmup stage ( $t > T_{\text{warm}}$ ), we transition to training on sampled subgraphs. This introduces two additional sources of variance: *Sampling Variance*: Due to sampling a subset of the graph with rate  $\rho$  and *Distribution Divergence*: Information loss from potentially missing important negative feedback.

Let's denote the true gradient as  $\nabla \mathcal{L}$  and the sampled gradient as  $\tilde{\nabla} \mathcal{L}$ . The variance of the sampled gradient can be decomposed as:

$$\begin{aligned} \text{Var}(\tilde{\nabla} \mathcal{L}) &= \mathbb{E} \|\tilde{\nabla} \mathcal{L} - \nabla \mathcal{L}\|_2^2 + \mathbb{E} \|\nabla \mathcal{L} - \mathbb{E}[\nabla \mathcal{L}]\|_2^2 \\ &= \underbrace{\frac{\sigma_0^2}{\rho}}_{\text{base variance}} + \underbrace{\frac{\kappa}{\rho^2}}_{\text{sparsity penalty}} + \underbrace{\nu(\rho)}_{\text{information loss}}, \end{aligned} \quad (32)$$

where  $\sigma_0^2$  is the base variance from full-graph training,  $\kappa$  is a constant that scales the variance inflation from rare negative feedback and  $\nu(\rho)$  measures the information loss due to potential systematic bias in sampled graphs.

The embedding difference now satisfies:

$$\begin{aligned} \mathbb{E} \|\mathbf{e}_v^{(t)} - \mathbf{e}_v^{(t-1)}\|_2^2 &= \mathbb{E} \|\mathbf{e}_v - \eta_{t-1} \tilde{\nabla}_{\mathbf{e}_v} \mathcal{L}(\Theta^{(t-1)})\|_2^2 \\ &= \eta_{t-1}^2 \mathbb{E} \|\tilde{\nabla}_{\mathbf{e}_v} \mathcal{L}(\Theta^{(t-1)})\|_2^2 \end{aligned} \quad (33)$$

The expected squared norm of the sampled gradient can be decomposed as:

$$\begin{aligned} \mathbb{E} \|\tilde{\nabla}_{\mathbf{e}_v} \mathcal{L}(\Theta^{(t-1)})\|_2^2 &= \|\mathbb{E}[\tilde{\nabla}_{\mathbf{e}_v} \mathcal{L}(\Theta^{(t-1)})]\|_2^2 + \text{Var}(\tilde{\nabla}_{\mathbf{e}_v} \mathcal{L}(\Theta^{(t-1)})) \\ &= \|\nabla_{\mathbf{e}_v} \mathcal{L}(\Theta^{(t-1)}) - \beta(\rho)\|_2^2 + \text{Var}(\tilde{\nabla}_{\mathbf{e}_v} \mathcal{L}(\Theta^{(t-1)})) \end{aligned} \quad (34)$$

where  $\beta(\rho)$  represents the bias introduced by sampling, which has magnitude proportional to  $\sqrt{\nu(\rho)}$ .

Combining these results:

$$\begin{aligned} \mathbb{E} \|\mathbf{e}_v^{(t)} - \mathbf{e}_v^{(t-1)}\|_2^2 &\leq \eta_{t-1}^2 \left( L^2 + \frac{\sigma_0^2}{\rho} + \frac{\kappa}{\rho^2} \right) + \eta_{t-1} \sqrt{\nu(\rho)} \\ &= \frac{\eta_0^2}{t} \left( L^2 + \frac{\sigma_0^2}{\rho} + \frac{\kappa}{\rho^2} \right) + \frac{\eta_0}{\sqrt{t}} \sqrt{\nu(\rho)} \\ &= \frac{C_2(\rho)}{t} + \frac{\epsilon(\rho)}{\sqrt{t}} \end{aligned} \quad (35)$$

where  $C_2(\rho) = \eta_0^2 \left( L^2 + \frac{\sigma_0^2 + \kappa/\rho}{\rho} \right)$  and  $\epsilon(\rho) = \eta_0 \sqrt{\nu(\rho)}$ .

This demonstrates that the embedding differences decay as  $O(1/t)$  during the warmup phase and as  $O(1/t) + O(1/\sqrt{t})$  during the sampling phase. The additional  $O(1/\sqrt{t})$  term reflects the trade-off between sampling efficiency (parameter  $\rho$ ) and approximation quality (parameters  $\kappa$  and  $\nu$ ).  $\square$

## B Detailed Multi-Objective Loss Integration

This section provides comprehensive details on our training approach that integrates recommendation supervision, contrastive learning signals, and distribution alignment to effectively capture both types of feedback patterns.

---

**Algorithm 2:** SDCGCL Optimization Algorithm

---

**Input** :Positive graph  $\mathcal{G}^+$ , negative graph  $\mathcal{G}^-$ , total epochs  $T$ , warm-up epochs  $T_{warm}$ , hyperparameters  $\alpha, \beta, \lambda, \gamma, \eta_r$ , learning rate  $\eta$   
**Output** :Trained model parameters  $\Theta$   
 Initialize model parameters  $\Theta$  randomly;

```

for  $t = 1$  to  $T$  do
  if  $t \leq T_{warm}$  then
     $\mathcal{G}_s^- \leftarrow \mathcal{G}^-$ ; /* Full negative graph for warm-up */
  else
     $\mathcal{G}_s^- \leftarrow \text{PGRWSampling}(\mathcal{G}^-, \rho)$ ; /* Algorithm 1 */
  end
  for each mini-batch  $\mathcal{B}$  do
    /* Dual-channel embedding generation */
     $\mathbf{E}^+, \mathbf{Z}^+ \leftarrow \text{GraphEncoder}(\mathcal{G}^+, \mathcal{B})$ ;
     $\mathbf{E}^-, \mathbf{Z}^- \leftarrow \text{GraphEncoder}(\mathcal{G}_s^-, \mathcal{B})$ ;
    /* Multi-objective loss computation */
     $\mathcal{L}_{rec} \leftarrow (1 - \alpha)\mathcal{L}_{rec}^+(\mathbf{E}^+) + \alpha\mathcal{L}_{rec}^-(\mathbf{E}^-)$ ;
     $\mathcal{L}_{cl} \leftarrow (1 - \beta)\mathcal{L}_{cl}^+(\mathbf{E}^+, \mathbf{Z}^+) + \beta\mathcal{L}_{cl}^-(\mathbf{E}^-, \mathbf{Z}^-)$ ;
     $\mathcal{L}_{dist} \leftarrow \text{JS}(\mathbf{E}^+, \mathbf{E}^-)$ ; /* Jensen-Shannon divergence */
    /* Total loss with regularization */
     $\mathcal{L} \leftarrow \mathcal{L}_{rec} + \lambda(\mathcal{L}_{cl} + \gamma\mathcal{L}_{dist}) + \eta_r\|\Theta\|_2^2$ ;
    /* Parameter update */
     $\Theta \leftarrow \text{Adam}(\Theta, \nabla_\Theta \mathcal{L}, \eta)$ ;
  end
end
return  $\Theta$ 

```

---

### B.1 Recommendation Loss

We adopt Bayesian Personalized Ranking (BPR) loss across both channels. For positive channel:

$$\mathcal{L}_{rec}^+ = - \sum_{(u, i, j) \in \mathcal{O}^+} \ln \sigma(\hat{y}_{u, i} - \hat{y}_{u, j}) \quad (36)$$

where  $\mathcal{O}^+$  contains positive triplets  $(u, i, j)$  with user  $u$ , observed item  $i$ , and unobserved item  $j$ . Similarly, for the negative channel, we can obtain  $\mathcal{L}_{rec}^-$ , the overall recommendation loss combines both channels:

$$\mathcal{L}_{rec} = (1 - \alpha)\mathcal{L}_{rec}^+ + \alpha\mathcal{L}_{rec}^- \quad (37)$$

### B.2 Contrastive Loss

Following Equations 5 and 6, we apply InfoNCE loss within each channel. For positive channel:

$$\mathcal{L}_{cl}^+ = - \sum_{u \in \mathcal{U}} \ln \frac{\exp(sim(\mathbf{E}_u^+, \mathbf{Z}_u^+)/\tau)}{\sum_{v \in \mathcal{U}} \exp(sim(\mathbf{E}_u^+, \mathbf{Z}_v^+)/\tau)} - \sum_{i \in \mathcal{I}} \ln \frac{\exp(sim(\mathbf{E}_i^+, \mathbf{Z}_i^+)/\tau)}{\sum_{j \in \mathcal{I}} \exp(sim(\mathbf{E}_i^+, \mathbf{Z}_j^+)/\tau)} \quad (38)$$

where  $sim(\cdot, \cdot)$  is dot product similarity and  $\tau$  controls distribution sharpness. Similarly, for the negative channel, we can obtain  $\mathcal{L}_{cl}^-$ , the combined loss is:

$$\mathcal{L}_{cl} = (1 - \beta)\mathcal{L}_{cl}^+ + \beta\mathcal{L}_{cl}^- \quad (39)$$

### B.3 Distribution Alignment Loss

For Inter-Channel Distribution Alignment (Equations 7), we use Jensen-Shannon divergence:

$$\mathcal{L}_{dist} = \sum_{u \in \mathcal{U}} JS\left(\sum_{i \in \mathcal{N}_u^+} \frac{\mathbf{E}_u^+ \circ \mathbf{E}_i^{+\top}}{\|\mathcal{N}_u^+\|}, \sum_{i \in \mathcal{N}_u^-} \frac{\mathbf{E}_u^- \circ \mathbf{E}_i^{-\top}}{\|\mathcal{N}_u^-\|}\right) + \sum_{i \in \mathcal{I}} JS\left(\sum_{u \in \mathcal{N}_i^+} \frac{\mathbf{E}_u^+ \circ \mathbf{E}_i^{+\top}}{\|\mathcal{N}_i^+\|}, \sum_{u \in \mathcal{N}_i^-} \frac{\mathbf{E}_u^- \circ \mathbf{E}_i^{-\top}}{\|\mathcal{N}_i^-\|}\right) \quad (40)$$

where normalized interaction scores correspond to neighborhood aggregation terms and JS divergence serves as  $g^*(\cdot, \cdot)$ .

#### B.4 Joint Training Objective

The final training objective combines all three components with balanced weighting parameters:

$$\mathcal{L} = \mathcal{L}_{rec} + \lambda(\mathcal{L}_{cl} + \gamma\mathcal{L}_{dist}) + \eta\|\Theta\|_2^2 \quad (41)$$

where  $\lambda$  controls the overall contribution of the auxiliary objectives,  $\gamma$  weights the distribution alignment constraint, and  $\eta$  is the  $L_2$  regularization coefficient applied to model parameters  $\Theta$ .

During training, we implement a two-stage optimization strategy where the full negative graph  $\mathcal{G}^-$  is used for the initial  $T_{warm}$  epochs (warm-up stage), followed by our efficient Popularity-Guided Random Walk Sampling approach for subsequent epochs. This warm-up period establishes stable initial representations while the sampling stage significantly reduces computational costs without sacrificing model performance.

Empirically, we found that setting  $T_{warm} = 1$  provides sufficient initialization while minimizing overhead, enabling our model to achieve superior results with reduced training time. The sampling rate  $\rho$  controls the subgraph size and directly affects the efficiency-quality trade-off as demonstrated in Section 4.3. The complete optimization process is formally presented in Algorithm 2.

## C Detailed Experimental Setup

### C.1 Datasets

We evaluate our method on four publicly available recommendation datasets: Yelp (business reviews), Amazon (book reviews), and MovieLens (movie ratings) with varying scales, as detailed in Table 4. Following established conventions [42, 56, 43], we binarize all numerical ratings by considering scores  $\geq 4$  as *positive feedback* and scores  $< 4$  as *negative feedback*. Each dataset is rigorously partitioned into training, validation, and test sets using a 7:1:2 ratio to prevent data leakage and ensure reproducible evaluation.

Table 4: Statistics of datasets. #Pos/#Neg refers to the percentage of positive and negative samples.

Dataset	#Users	#Items	#Interaction	#Pos/#Neg
Yelp <sup>1</sup>	29,601	24,734	2,074,594	66.3%/33.7%
Amazon <sup>2</sup>	35,736	38,121	1,960,674	80.6%/19.4%
ML-1M <sup>3</sup>	6,040	3,706	1,000,209	57.5%/42.5%
ML-10M <sup>3</sup>	69,878	10,677	10,000,054	58.9%/41.1%

### C.2 Metrics

For performance evaluation, we adopt two standard ranking metrics: Recall@K, which measures the ratio of correctly recommended items over all ground truth items, and NDCG@K, which considers both the hit ratio and position of correctly recommended items. Following previous studies on graph-based recommendation [16, 2, 57, 6], we set K = 20 in our experiments.

### C.3 Baselines

In our experimental evaluation, we benchmark our SDCGCL framework against a diverse set of 22 contemporary recommendation methods. These approaches can be divided into two main categories.

- **Unsigned RS:** Traditional methods like **MF** [23] and **NCF** [15] focus on basic collaborative filtering. Graph-based approaches including **NGCF** [40], **LightGCN** [16], and **DGCF**

<sup>1</sup><https://business.yelp.com/data/resources/open-dataset/>

<sup>2</sup>[https://cseweb.ucsd.edu/~jmcauley/datasets/amazon\\_v2/](https://cseweb.ucsd.edu/~jmcauley/datasets/amazon_v2/)

<sup>3</sup><https://grouplens.org/datasets/movielens/>

[41] leverage various graph neural architectures. Advanced frameworks such as **HyRec** [38], **GFormer** [24], and **SelfGNN** [28] explore specialized structures. Recent contrastive learning methods (**NCL** [27], **SGL** [46], **LightGCL** [2], **XSimGCL** [57], **IGCL** [13]) enhance representation learning through different augmentation strategies.

- **Sign-aware RS:** Early approaches (**SiReN** [34], **SiGRec** [21], **DFGNN** [49]) focus on separate processing of positive and negative feedback. Transformer-based methods including **SignGT** [4], **SGFormer** [47], and **SIGformer** [6] leverage attention mechanisms. Other specialized architectures like **SBGNN** [20], **SLGNN** [25], and **NFARec** [43] explore unique graph structures and operators for signed feedback.

#### C.4 Experiment Setting

For our SDCGCL, we adopt the Adam optimizer and employ grid search for hyperparameter optimization. Specifically, we set the hidden embedding dimension  $d$  to 64. The learning rate is set to  $10^{-3}$  with a batch size of 2048. The hyperparameter search ranges are  $\alpha \in [0, 1]$ ,  $\beta \in [0, 1]$ ,  $\gamma \in [0, 1]$ ,  $k \in [0, 1]$  and  $\lambda \in [0.05, 0.35]$ . For computational efficiency,  $T_{warm}$  is uniformly set to 1. For other baseline models, we strictly follow their officially released code to ensure fair comparison. All experiments in this paper are conducted on 8 RTX3090 GPUs.

## D Additional Experiments

### D.1 Computational Efficiency Analysis

Our SDCGCL framework introduces minimal computational overhead (3-8s per epoch) while significantly improving convergence speed across different base models. SDCGCL-DualFuse achieves the best efficiency with the fastest convergence (21 epochs) and lowest total training time (20.8 minutes) on ML-1M dataset, benefiting from both the enhanced learning signals of negative feedback and efficient architecture design. Compared to the base models (SGL, LightGCL, XSimGCL), our framework consistently reduces the overall training time by improving convergence despite the slight increase in per-epoch processing time.

We provide a detailed analysis of the time complexity for our framework and its comparison with other methods.

Table 5: Runtime comparison across methods on ML-1M dataset.

Method	Time/epoch	Epochs	Total time
SGL	81.09s	32	43.25m
SDCGCL-SGL	89.57s	27	40.31m
LightGCL	66.09s	23	25.3m
SDCGCL-LightGCL	69.57s	24	27.83m
XSimGCL	<b>56.09s</b>	25	23.3m
SDCGCL-XSimGCL	59.34s	23	22.74m
SDCGCL-DualFuse	59.57s	<b>21</b>	<b>20.8m</b>

Table 6: Detailed time complexity comparison across methods.  $q$ : preserved features in LightGCL SVD;  $a$ : augmentation ratio in SGL;  $\rho_0$ : the two-stage optimization weighting coefficient;  $\mathcal{M} = |\mathcal{U}| + |\mathcal{I}|$ : total nodes.

Method	Augmentation	Convolution	BPR	Contrast	Align	Time/Epoch
SGL	$O(2a \mathcal{E}^+ )$	$O(2 \mathcal{E}^+ Ld + 4a \mathcal{E}^+ Ld)$	$O(2\mathcal{M}d)$	$O(\mathcal{M}d)$	-	81.09s
SDCGCL-SGL	$O(2a \mathcal{E}^+  + 2a\rho_0 \mathcal{E}^- )$	$O((2 + 4a)( \mathcal{E}^+  + \rho_0 \mathcal{E}^- )Ld)$	$O(2\mathcal{M}d)$	$O(\mathcal{M}d)$	$O(\mathcal{M}d)$	89.57s
LightGCL	-	$O(2 \mathcal{E}^+ Ld + 2q\mathcal{M}Ld)$	$O(2\mathcal{M}d)$	$O(\mathcal{M}d)$	-	66.09s
SDCGCL-LightGCL	-	$O(2( \mathcal{E}^+  + \rho_0 \mathcal{E}^- )Ld + 4q\mathcal{M}Ld)$	$O(2\mathcal{M}d)$	$O(\mathcal{M}d)$	$O(\mathcal{M}d)$	69.57s
XSimGCL	-	$O(2 \mathcal{E}^+ Ld)$	$O(2\mathcal{M}d)$	$O(\mathcal{M}d)$	-	<b>56.09s</b>
SDCGCL-XSimGCL	-	$O(2 \mathcal{E}^+ Ld + 2\rho_0 \mathcal{E}^- Ld)$	$O(2\mathcal{M}d)$	$O(\mathcal{M}d)$	$O(\mathcal{M}d)$	59.34s
SDCGCL-DualFuse	-	$O(2 \mathcal{E}^+ Ld + 2\rho_0 \mathcal{E}^- Ld)$	$O(2\mathcal{M}d)$	$O(\mathcal{M}d)$	$O(\mathcal{M}d)$	59.57s

As a preprocessing step, SDCGCL employs a negative graph sampling strategy with complexity  $O(k\rho\mathcal{M})$ , where  $k$  denotes the number of sampled neighbors and  $\rho$  represents the sampling ratio. We define  $\rho_0$  as the two-stage optimization weighting coefficient, whose value is  $(epoch - T_{warm})\rho + T_{warm}$ . Since  $T_{warm} = 1 \ll epoch$ , therefore  $\rho_0 \approx \rho$ .

The additional computational overhead introduced by SDCGCL varies across different base models, with complexity  $O(2\rho_0|\mathcal{E}^-|Ld)$  for XSimGCL,  $O(2q\mathcal{M}Ld)$  for LightGCL, and  $O(2a\rho_0|\mathcal{E}^-|Ld)$  for SGL. DualFuse, specifically designed for efficient implementation of the SDCGCL framework, maintains the same simplified convolution complexity  $O(2|\mathcal{E}^+|Ld + 2\rho_0|\mathcal{E}^-|Ld)$  as SDCGCL-XSimGCL while avoiding additional operations like feature decomposition or augmentation required by other variants.

The theoretical analysis of time complexity can only reveal the complexity of each epoch, while the actual running time is also affected by factors such as convergence speed. Our empirical results in Table 5 demonstrate that SDCGCL framework consistently improves training efficiency across different base models by introducing minimal computational overhead while significantly accelerating convergence in most cases.

## D.2 Performance Gains Analysis

Table 7 presents a comprehensive analysis of performance enhancements achieved by the SDCGCL framework when integrated with existing recommendation approaches. The empirical evidence demonstrates consistent and substantial improvements across multiple datasets and baseline architectures.

Table 7: Performance enhancement analysis of the SDCGCL framework relative to baseline models. Results are reported as Recall@20/NDCG@20 pairs, with improvement percentages indicating relative performance gains across metrics.

Dataset	Base Model	Original	SDCGCL-Enhanced	Improvement (%)
ML-1M	SGL	0.2798/0.3037	0.2879/0.3300	+2.89%/+8.66%
	LightGCL	0.2730/0.3035	0.2945/0.3423	+7.88%/+12.78%
	XSimGCL	0.2729/0.3087	0.3050/0.3401	+11.76%/+10.17%
Yelp	SGL	0.0746/0.0729	0.1136/0.0907	+52.28%/+24.42%
	LightGCL	0.0697/0.0675	0.1069/0.0826	+53.37%/+22.37%
	XSimGCL	0.0867/0.0758	0.1112/0.0881	+28.26%/+16.23%
Amazon	SGL	0.0958/0.0694	0.1108/0.1001	+15.66%/+44.24%
	LightGCL	0.0967/0.0728	0.1057/0.0890	+9.31%/+22.25%
	XSimGCL	0.0963/0.0707	0.1142/0.1014	+18.59%/+43.42%
ML-10M	SGL	0.3056/0.3299	0.3768/0.3716	+23.30%/+12.64%
	LightGCL	0.3098/0.3231	0.3810/0.3760	+22.98%/+16.37%
	XSimGCL	0.3109/0.3371	0.3791/0.3726	+21.94%/+10.53%

## D.3 Extended Ablation Analysis

We evaluate the contribution of each key component by conducting ablation studies on: (1) cross-channel fusion ("w/o Fusion") from the DualFuse base model, and three components from our SDCGCL framework: (2) contrastive learning ("w/o CL"), (3) distribution alignment ("w/o Align"), and (4) recommendation loss ("w/o Rec"). Figure 4 and Table 8 present the visualization and quantitative results across all datasets. The experimental results reveal that cross-channel fusion

Table 8: Ablation study on different components of SDCGCL. The base model is the DualFuse. Best results are highlighted in **bold**.

Variant	ML-1M		Yelp		Amazon		ML-10M	
	Recall	NDCG	Recall	NDCG	Recall	NDCG	Recall	NDCG
DualFuse	<b>0.3282</b>	<b>0.3693</b>	<b>0.1243</b>	<b>0.0959</b>	<b>0.1342</b>	<b>0.1113</b>	<b>0.3900</b>	<b>0.3860</b>
w/o Fusion	0.0860	0.0857	0.1046	0.0894	0.1274	0.1063	0.1624	0.1494
w/o CL	0.2983	0.3307	0.0969	0.0835	0.1161	0.0950	0.3780	0.3699
w/o Align	0.3231	0.3564	0.1032	0.0896	0.1297	0.1086	0.3847	0.3751
w/o Rec	0.2436	0.2586	0.0793	0.0667	0.0680	0.0530	0.1535	0.1389

exhibits dataset-dependent impact. Its removal causes severe performance degradation on MovieLens (73.80% decrease in Recall@20 on ML-1M, 58.36% decrease on ML-10M) but moderate impact on Yelp (15.85% decrease) and minimal impact on Amazon (5.07% decrease). This suggests that cross-channel fusion is particularly critical for datasets with dense user-item interaction patterns like MovieLens.

The contrastive learning component consistently contributes to model performance across all datasets, with its removal causing 10.45% decrease in NDCG@20 on ML-1M, 12.93% on Yelp, 14.65% on Amazon, and 4.17% on ML-10M. Similarly, distribution alignment shows moderate but consistent impact across datasets, with performance drops of 3.49% on ML-1M, 6.57% on Yelp, 2.43% on Amazon, and 2.82% on ML-10M when removed.

Most importantly, the recommendation loss proves essential for effective training across all datasets, as its removal leads to randomly scattered embedding distributions (Figure 4(e)) and the most substantial performance drops: 69.94% decrease in NDCG@20 on ML-1M, 30.45% on Yelp, 52.38% on Amazon, and 64.02% on ML-10M. This demonstrates the fundamental role of supervised signals in learning discriminative representations for different types of feedback, regardless of dataset characteristics.

## E Limitations and Future Work

While our proposed SDCGCL framework demonstrates significant improvements across multiple benchmarks, there are several avenues for future exploration. The current implementation has been validated on public benchmark datasets, but deployment in large-scale industrial recommender systems might introduce additional complexities that deserve further investigation. Additionally, the framework could be extended to capture dynamic evolution of user feedback patterns over time, which might further enhance recommendation performance in dynamic environments. Future work could also explore the integration of explicit explanation mechanisms to improve user experience and trust, as well as adaptation strategies for extreme cold-start scenarios where both positive and negative feedback signals are initially limited.

## F Broader Impacts

Our work focuses on enhancing both the performance and efficiency of recommender systems through effective utilization of negative feedback, thereby benefiting the overall development of recommendation technologies. The proposed framework improves user experience across various digital platforms including e-commerce, social media, and content streaming services. We do not foresee any negative impacts resulting from our work.